Changes of urinary proteome in high-fat diet *ApoE*$^{-/-}$ mice

Hua Yuanrui, Meng Wenshu, Wei Jing, Liu Yongtao & Gao Youhe*
College of Life Sciences, Beijing Normal University, GeneEngineering Drug and Biotechnology Beijing Key Laboratory, Beijing, China

Abstract

Cardiovascular disease is currently the leading cause of death worldwide. Atherosclerosis is an important pathological basis of cardiovascular disease, and its early diagnosis is of great significance. Urine is more conducive in the accumulation and response of changes in the physiological state of the body and is not regulated by homeostasis mechanisms, so it is a good source of biomarkers in the early stage of disease. In this study, *ApoE*$^{-/-}$ mice were fed with a high-fat diet for 5 months. Urine samples from the experimental group and control group, which were C57BL/6 mice fed a normal diet, were collected at seven time points. Proteomic analysis was used for internalcontrol and intergroup control. Internal control results showed a significant difference in the urinary proteome before and after a 1-week high-fat diet, and several differential proteins have been reported to be associated with atherosclerosis or for use as candidate biomarkers. The results of the intergroup control indicated that the biological process enriched by the GO analysis of the differential proteins corresponded to the progression of atherosclerosis. Differences in chemical modifications of urinary proteins have also been reported to be associated with the disease. This study demonstrates that urinary proteomics has the potential to monitor changes in the body sensitively and provides the possibility of identifying early biomarkers of atherosclerosis.

Key Words: *ApoE*$^{-/-}$ mice; High-fat diet; Urinary proteome; Chemical modifications; Early biomarker

1 Introduction

Atherosclerosis (AS) is the primary pathological basis of cardiovascular disease (CVD)[1], which is the leading cause of death in the world today[2]. In 2015, more than 17 million people died of cardiovascular disease, accounting for 31% of all deaths worldwide[3]. The impact of atherosclerosis is more significant during the late stages and induces a series of fatal consequences, such as myocardial infarction and stroke. Therefore, its early diagnosis is of vital importance.

Urine is an ideal source of early biomarkers because biomarkers are measurable changes related to biological processes regulated by homeostasis mechanisms, and urine can accumulate these early changes [4]. This conclusion has been confirmed by many related studies. For example, in a glioblastoma animal model constructed by injecting tumour cells into the brains of rats, changes in the urine proteome occurred before magnetic resonance imaging reflected the changes caused by the tumour [5]. Similarly, studies have confirmed that even if only approximately 10 cells are subcutaneously inoculated in rats, the urinary proteome can also change significantly [6]. In addition, urine is more accessible and non-invasive to obtain.

The use of animal models avoids the influence of genetic, environmental and other factors on the urinary proteome, and it is easier to judge the early stage of atherosclerosis and identify biomarkers [7]. Apolipoprotein E (*ApoE*) plays an important role in maintaining the normal levels of

cholesterol and triglycerides in serum by transporting lipids in the blood [8]. Mice lacking *ApoE* function develop hypercholesterolemia, increased very-low-density lipoprotein (VLDL) and decreased high-density lipoprotein (HDL), exhibiting spontaneous formation of plaques, and a high-fat diet can greatly accelerate the formation of plaques [9].

In this experiment, *ApoE*$^{-/-}$ mice were fed with a 5-month high-fat diet. At different timepoints (week 0, week 1, month 1, month 2, month 3, month 4, and month 5) of the experimental process, urine samples were collected and analysed by mass spectrometry. Internal control of the results was conducted as well as intergroup control using urine samples of normal diet C57BL/6 mice. The changes in the proteome and chemical modifications that occur during disease progression provide clues in the search for biomarkers.

2 Materials and methods

2.1 Experimental animals

Six 4-week-old male *ApoE*$^{-/-}$ mice were purchased from the Laboratory Animal Science Department of Peking University Health Science Centre and fed a high-fat diet (21% fat and 0.15% cholesterol, Beijing Keao Xieli Feed Co., Ltd.) for 5 months. The animal licence is SCXK (Beijing) 2016-0010. A 12-hour normal light-dark cycle and standard temperature (22°C±1°C) and humidity (65%-70%) conditions were used. All animal protocols governing the experiments in this study were approved by the Institute of Basic Medical Sciences Animal Ethics Committee, Peking Union Medical College (Approved ID: ACUC-A02-2014-007). The study was carried out in compliance with the ARRIVE guidelines.

2.2 Histopathology

Six 6-month-old *ApoE*$^{-/-}$ mice in the experimental group and four 6-month-old normal diet C57BL/6 mice (purchased from Beijing Vital River Laboratory Animal Technology Co., Ltd.) were euthanized together. Whole arteries were dissected and stained with Oil Red O [10]. The aorta was fixed in 4% paraformaldehyde and dehydrated with isopropanol. After longitudinal incision, it was stained with Oil Red O dye solution (Biotopped, China) for 20 minutes and rinsed three times with isopropanol. A digital camera (Canon, Japan) was then used to obtain images of the aorta, which were analysed using ImageJ software (1.52a, NIH, USA).

2.3 Urine collection and sample preparation

To identify the short-term effects of a high-fat diet on animals, urine samples of experimental group mice in week 0 and week 1 were collected during the experiment. To monitor changes in the urinary proteome during the whole process, urine samples of the experimental group at months 1, 2, 3, 4 and 5 were also collected. The urine of four C57BL/6 mice fed a normal diet (all purchased from Beijing Vital River Laboratory Animal Technology Co., Ltd.) corresponding to the age of *ApoE*$^{-/-}$ mice was collected as a control group (not the same batch). All mice were placed in metabolic cages individually for 12 h to collect urine without any treatment. The collected urine samples were immediately stored at -80°C. The experimental process is shown in Figure 1.

The urine samples were centrifuged at 12,000 g for 40 minutes to remove the supernatant, precipitated using 3 times the volume of ethanol overnight, and then centrifuged at 12,000 g for 30 minutes. The protein was resuspended in lysis buffer (8 mol/L urea, 2 mol/L thiourea, 25 mmol/L

dithiothreitol and 50 mmol/L Tris). The protein concentration was measured using the Bradford method. Urine proteolysis was performed using the filter-aided sample preparation (FASP) method[11]. The urine protein was loaded on the filter membrane of a 10 kDa ultrafiltration tube (PALL, USA) and washed twice with UA (8 mol/L urea, 0.1 mol/L Tris-HCl, pH 8.5) and 25 mmol/L NH_4HCO_3 solution; 20 mmol/L dithiothreitol (DTT, Sigma, USA) was added for reduction at 37°C for 1 hour, and then 50 mmol/L iodoacetamide (IAA, Sigma, USA) was used for alkylation in the dark for 30 minutes. After washing twice with UA and NH_4HCO_3 solutions, trypsin (Promega, USA) was added at a ratio of 1:50 for digestion at 37°C for 14 hours. The peptides were passed through Oasis HLB cartridges (Waters, USA) for desalting and then dried by vacuum evaporation (Thermo Fisher Scientific, Germany).

2.4 Spin column peptide fractionation

The digested samples were redissolved in 0.1% formic acid and diluted to 0.5 μg/μL. Each sample was used to prepare a mixed peptide sample, and a high pH reversed-phase fractionation spin column (Thermo Fisher Scientific) was used for separation. The mixed peptide samples were added to the chromatographic column and eluted with a step gradient of 8 increasing acetonitrile concentrations (5, 7.5, 10, 12.5, 15, 17.5, 20 and 50% acetonitrile). Ten effluents were finally collected by centrifugation, dried with vacuum evaporation and resuspended in 0.1% formic acid. In this study, iRT reagent (Biognosis, Switzerland) was used to calibrate the retention time of the extracted peptide peaks, which were added to ten components and each sample at a volume ratio of 10:1.

2.5 LC-MS/MS analysis

An EASY-nLC 1200 chromatography system (Thermo Fisher Scientific) and Orbitrap Fusion Lumos Tribrid mass spectrometer (Thermo Fisher Scientific) were used for mass spectrometry acquisition and analysis. The peptide sample was loaded onto the precolumn (75 μm×2 cm, C18, 2 μm, Thermo Fisher) at a flow rate of 400 nL/min and then separated using a reversed-phase analysis column (50 μm×15 cm, C18, 2 μm, Thermo Fisher) for 120 minutes. The mobile phase with a gradient of 4%-35% (80% acetonitrile + 0.1% formic acid + 20% water) was used for elution. A full MS scan was acquired within a 350-1,500 m/z range with the resolution set to 120,000. The MS/MS scan was acquired in Orbitrap mode with a resolution of 30,000. The HCD collision energy was set to 30%. The mass spectrum data of 10 components separated by the reversed-phase column and all the samples obtained by enzymatic hydrolysis were collected in DDA mode.

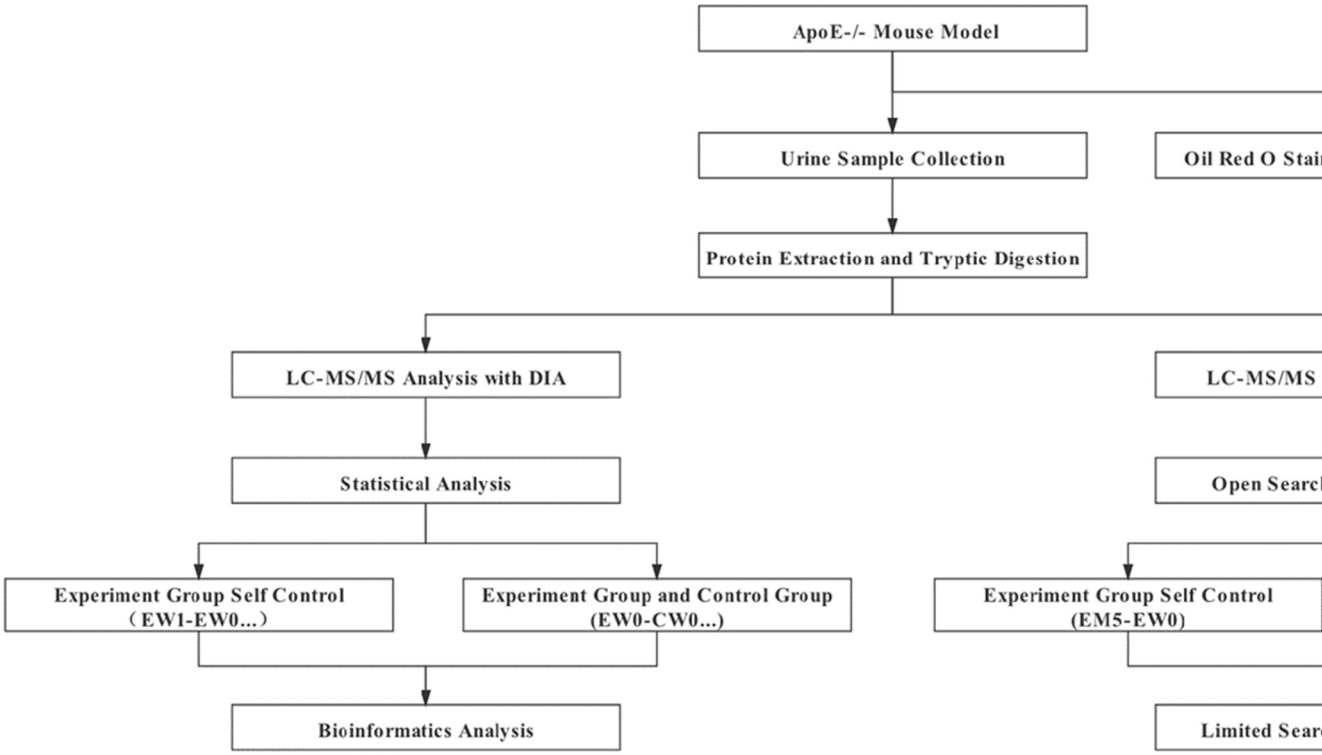

Figure 1 Experimental flow graph

2.6 Label-free DIA quantification

The DDA collection results of the above 10 components were imported into the Proteome Discoverer software (version 2.1, Thermo Scientific) search database using the following parameters: mouse database (released in 2019, containing 17038 sequences) with the iRT peptide sequence attached, trypsin digestion, a maximum of two missing cleavage sites are allowed, parent ion mass tolerance is 10 ppm, fragment ion mass tolerance is 0.02 Da, set methionine oxidation as variable modification, set cysteine carbamidomethylation as fixed modification, and protein false discovery rate (FDR) is set to 1%. The PD search result was used to establish the DIA acquisition method and the window width and number were calculated according to the m/z distribution density.

Sixty-nine peptide samples were put into DIA mode to collect mass spectrometry data. Spectronaut™ Pulsar X (Biognosys, Switzerland) software was used to process and analyse mass spectrometry data [12]. According to the DDA search result pdResult file and 10 DDA raw files, create a spectrum library, the raw files collected by DIA were imported for each sample to search the library. The high-confidence protein standard was a peptide q value<0.01, and the peak area of all fragment ions of the secondary peptide was used for protein quantification.

2.7 Protein chemical modifications search

PFind Studio software (version 3.1.6, Institute of Computing Technology, Chinese Academy of Sciences) was used to perform label-free quantitative analysis of the DDA collection results of enzymatic hydrolysis samples [13]. The target search database was from the *Mus musculus* database downloaded by UniProt (updated to September 2020). During the search process, the instrument type was set as HCD-FTMS, the enzyme was fully specific trypsin, and up to 2 missed cleaved sites were allowed. The "open-search" mode was selected, and the screening condition was that the FDR at the peptide level was less than 1%. The data used both forward and reverse database search strategies to analyse the data. After the initial screening, a restricted search method was used for verification.

2.8 Statistical analysis

The missing abundance values were determined (KNN method) [14], and CV value screening (CV<0.3) [15] was performed on the mass spectrometry results. The two-sided unpaired t-test was used for the comparison between each set of data. The internal control of the experimental group and the intergroup control at the same time points were screened for differential proteins. The screening criteria were as follows: fold change (FC) between the two groups ≥1.5 or ≤0.67 and p <0.05. At the same time, the samples in each two groups were randomly combined, and the average number of differential proteins in all permutations and combinations was calculated according to the same criteria as normal screening (Table S1), ensuring that differential proteins were generated by differences between groups rather than random production.

The proportions of different types of chemical modification sites in the total modification sites were calculated, and the data between each two groups were compared by two-sided unpaired t-tests. The screening criteria were FC between the two groups ≥1.5 or ≤0.67 and p <0.05.

The DAVID database (https://david.ncifcrf.gov) [16] was used to perform functional enrichment analysis on the differential proteins that were screened. The significance threshold of p <0.05 was

adopted. All methods were performed in accordance with the relevant guidelines and regulations.

3 Results and Discussion

3.1 Histopathology

The Oil Red O staining results of the whole aorta of 6-month-old *ApoE*$^{-/-}$ mice fed a high-fat diet for 5 months were compared to those of 6-month-old mice fed a normal diet. The average percentage of stained areas in the experimental group was 17.78±2.14% (n=6), and the average percentage in the control group was 0.88±0.34% (n=4), p=0.0004 (Figure 2).

a

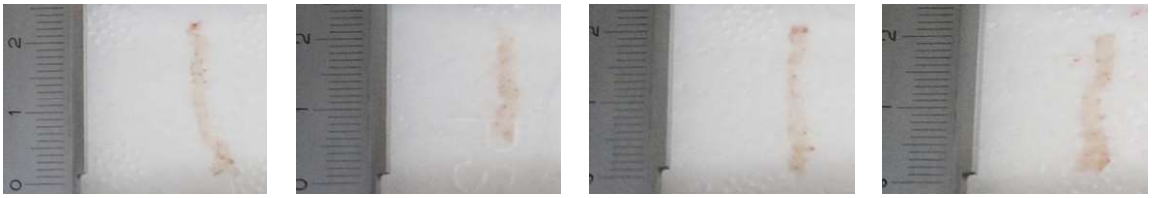

b

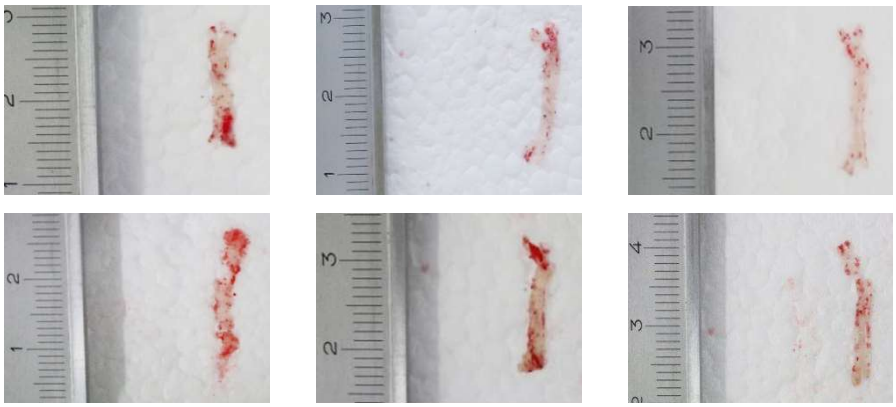

c

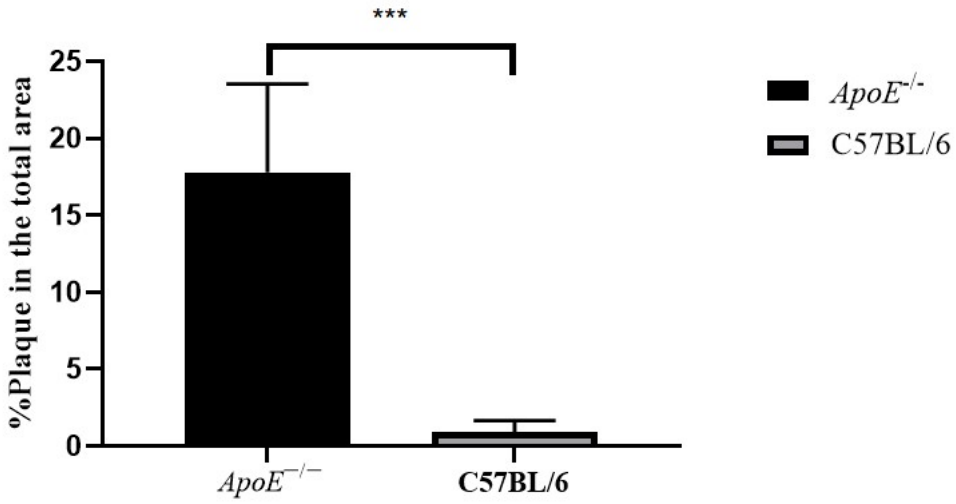

Figure 2 Results and quantitative analysis of oil red O staining of the whole aorta.

(a) Results of oil red O staining in the control group; (b) Results of oil red O staining in the experimental group; (c) The comparison of the staining area ratio.

3.2 Differential proteins screening and functional annotation

The experimental group and the control group had 69 samples from seven time points (W0/W1/M1/M2/M3/M4/M5) for non-labelled LC-MS/MS quantification (one sample in the experimental group on W0 was insufficient). A total of 592 proteins identified with at least 2 unique peptides with FDR<1% were identified, and an average of 360 urine proteins were identified for each sample. The mass spectrometry proteomics data have been deposited to the ProteomeXchange Consortium (http://proteomecentral.proteomexchange.org) via the iProX partner repository[17] with the dataset identifier PXD027610.

3.2.1 Internal control of the experimental group

(1) Short-term effects of a high-fat diet

To identify the effects of a high-fat diet, after a week of a high-fat diet in *ApoE*$^{-/-}$ mice, urine samples collected from W0 and W1 were compared and analysed. A total of 12 proteins were significantly upregulated and 15 proteins were significantly downregulated at W1 (Table 1). Among them, 21 proteins or their family members have been reported to be associated with lipids.

GO analysis of these 27 proteins by DAVID showed that most of the annotated biological processes were related to lipid metabolism and glucose metabolism (Figure 3). At the same time, the differential proteins between W1 and W0 in the control group (Table S2) did not enrich for any significant changes in biological processes, indicating that the physiological state of mice did not change significantly at W1, while even a week of a high-fat diet induced huge changes in the animal urinary proteome, further demonstrating that the urinary proteome sensitively reflects changes in the body.

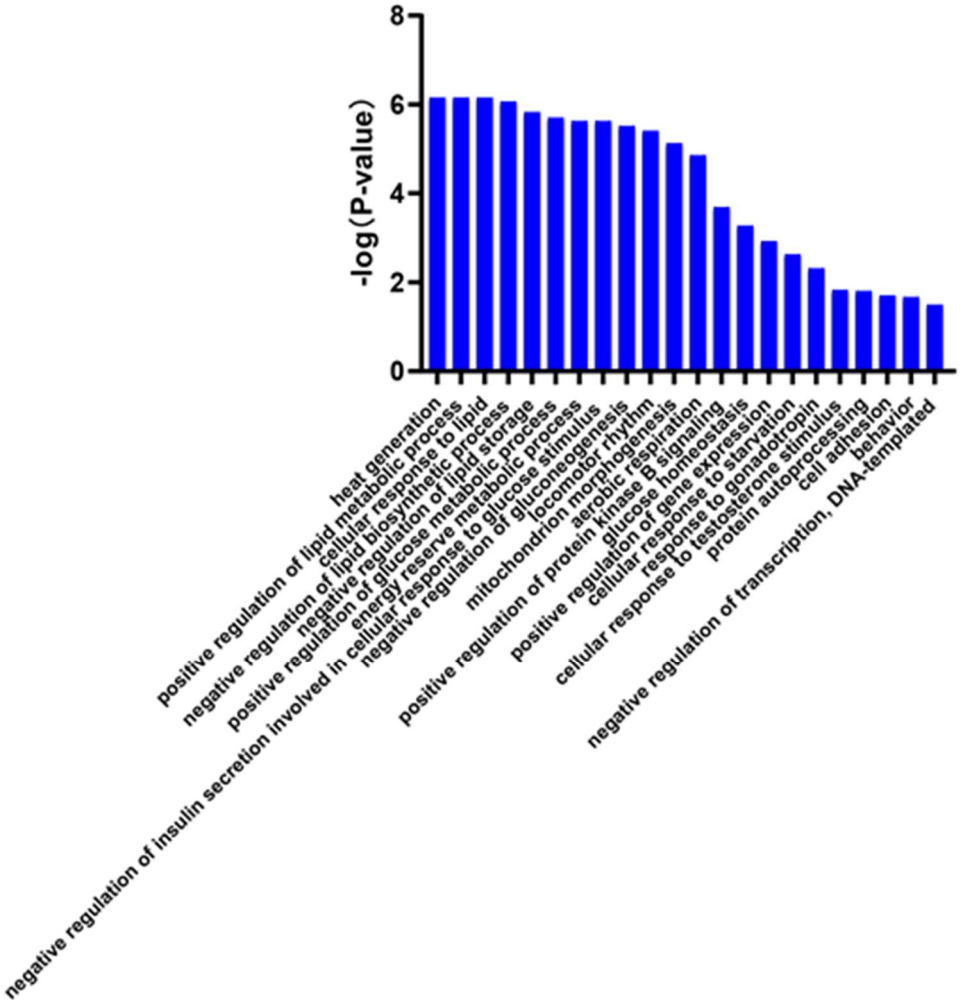

Figure 3 Biological processes enriched in differential proteins between week 1 and week 0 samples of the experimental group (p <0.05).

(2) Urinary proteome changes in whole process

Compared to W0, 51/69/86/65/88 proteins changed significantly at M1/M2/M3/M4/M5 in the experimental group, respectively. The Venn diagram (Figure 4) shows that a total of 17 proteins changed significantly at all five time points, and the DIA quantitative results show that these 17 proteins exhibited the same change trend at these time points. Another 18 proteins changed significantly at the last four time points, and the trend of change was the same at each time point (Table S3). Among them, 26 proteins or their family members have been previously reported to be related to lipid metabolism or cardiovascular diseases.

Major urinary proteins (MUPs) are members of the lipocalcin family, which can be isolated and transport various lipophilic molecules in the blood and other body fluids [18]. Knockout of mouse trefoil factor 2 protects against obesity in response to a high-fat diet [19]. Angiotensinogen plays a key role in fat cell metabolism and inflammation development [20]. Alpha1-antitrypsin has been reported as a biomarker of atherosclerosis [21]. It has been reported that CCN4 promotes the migration and proliferation of vascular smooth muscle cells by interacting with α5β1 integrin [22], which plays a vital role in the occurrence and development of atherosclerosis. Regular monitoring of vitamin B12 status may help prevent atherosclerosis-related diseases, and anticobalamin 2 can

carry vitamin B12 [23]. Regenerated islet-derived protein 3β, an inflammatory marker, is of great significance for the recruitment of macrophages and tissue repair [24]. The level of α-2-HS-glycoprotein is positively correlated with atherosclerotic substitution parameters, such as intima-media thickness (IMT) and arteriosclerosis [25]. The literature shows that gelsolin stabilizes actin filaments by binding to the ends of filaments, preventing monomer exchange. Its downregulation indicates that the cytoskeleton of vascular smooth muscle cells in the human coronary atherosclerotic medium is dysregulated [26]. It has been reported that *SCUBE2* may play an important role in the progression of atherosclerotic plaques through Hh signal transduction [27]. Type I collagen is an early biomarker of atherosclerosis [21].

Igκ chain V-III region PC 7043, Igκ chain V-II region 26-10 and immunoglobulin κ constant are all involved in the adaptive immune response. The haptoglobin polymorphism is related to the prevalence and clinical evolution of many inflammatory diseases, including atherosclerosis [28]. MHCII antigen presentation has an important protective function in atherosclerosis [29]. Interleukin-18 plays a key role in atherosclerosis and plays a role in appetite control and the development of obesity [30]. According to the literature, compared to healthy controls, *LAMP-2* gene expression and protein levels in peripheral blood leukocytes of patients with coronary heart disease are significantly increased [31]. T-cadherin is essential for the accumulation of adiponectin in neointima and atherosclerotic plaque lesions [32]. Kidney androgen-regulated protein has also been reported in the urine of *ApoE*$^{-/-}$ mice fed a high-fat diet [21]. Fibronectin is an indicator of connective tissue formation during atherosclerosis [33]. Peripheral arterial occlusive disease (PAOD) is one of the primary manifestations of systemic atherosclerosis, and transthyretin and complement factor B are potential markers for monitoring plasma PAOD disease [34]. Serotransferrin plays an important role in atherosclerosis [35]. The differential expression of serine protease inhibitor A3 in blood vessels is significantly related to human atherosclerosis [36]. Prolactin plays a role in the proliferation of vascular smooth muscle cells, and the proliferation of vascular smooth muscle cells is a characteristic of cardiovascular diseases, such as hypertension and atherosclerosis [37].

a

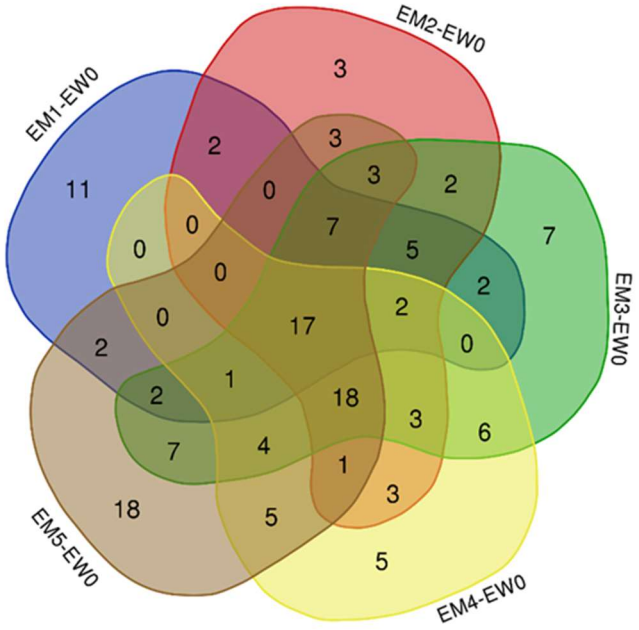

b

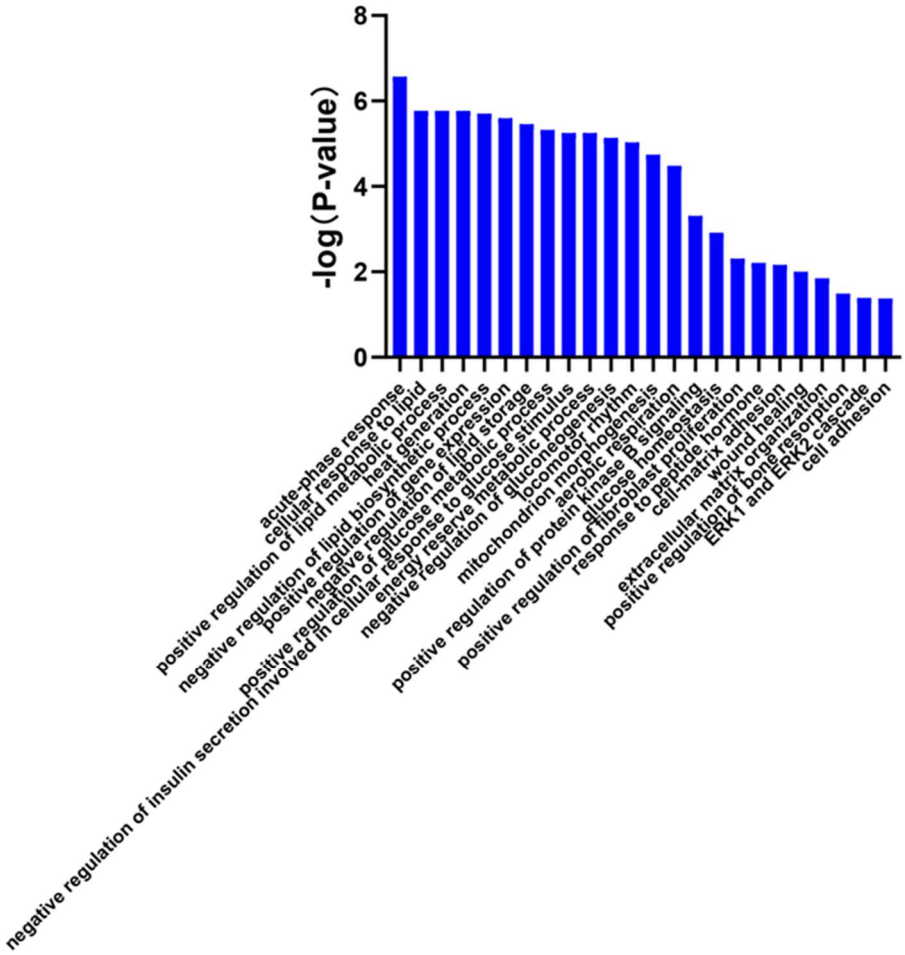

Figure 4 Differential proteins in the whole process.

(a) Venn diagram of differential proteins among the other time points (M1/M2/M3/M4/M5) and week 0 samples in the experimental group. (b) Biological processes enriched by continuously changing proteins in the internal control of the experimental group ($p < 0.05$).

The abovementioned differential proteins that continually changed during the whole process were analysed using DAVID for GO analysis (Figure 4), and the enriched biological processes are also shown in the figure.

The major urinary protein-induced lipid metabolism and glucose metabolism-related biological processes changed significantly; the acute phase reaction has been reported in the literature to be related to atherosclerosis [38]. The positive regulation of fibroblast proliferation also changed significantly, and vascular damage and dysfunction of adipose tissue around blood vessels promotes vasodilation, fibroblast activation and myofibroblast differentiation [39]. Wound healing is also related to atherosclerosis [40]. The extracellular matrix gives atherosclerotic lesion areas tensile strength, viscoelasticity, and compressibility [41], There are also reports showing a correlation between osteoporosis and atherosclerosis [42]. The ERK1/ERK2 pathway is involved in insulin (INS)

and thrombin-induced vascular smooth muscle cells, which play important roles in proliferation [43]. Cell adhesion also plays an important role in atherosclerosis [44].

The internal control of the experimental group avoids the influence of genetic and dietary differences on the experimental results to the greatest extent, but the influence of biological growth and development is difficult to avoid. The results show that there are a variety of proteins that change continually throughout the progression of the disease and are closely related to the disease. It is worth noting that the differential proteins obtained using this comparison method, and the biological processes and pathways enriched by them exhibited a high degree of overlap at different time points, which may be difficult in enhancing the early diagnosis of the disease, so follow-up intergroup control was performed.

3.2.2 Intergroup control

The comparison of the results between the experimental group and the control group at the same time points showed that 44/16/54/23/48/57/46 differential proteins were obtained at W0/W1/M1/M2/M3/M4/M5, respectively. The details of proteins are shown in Table 2, and the overlap of differential proteins at different time points is shown in Figure S1. Under intergroup control conditions, there were significant differences in the differential proteins at each time point, but they were all closely related to lipids and cardiovascular diseases.

The differential proteins were analysed by DAVID for GO analysis, and the biological processes that changed significantly at different time points are shown in Figure 5. The biological processes related to lipid metabolism and glucose metabolism in the experimental group were significantly different from those in the control group at W0. At W0 and M4, the immune-related processes were significantly different. Differential proteins at M1 were primarily enriched in cell adhesion-related processes, while at M2, they were primarily enriched in redox reaction-related processes. At M3, wound healing began to appear, and there were many adhesion-related processes. In addition to a large number of immune-related processes, the positive regulation of fibroblast proliferation and the negative regulation of angiogenesis also appeared at M4. The processes related to phagocytosis and proteolysis began to appear at M5.

(1) Effects of genetic factors

At W0, before a high-fat diet was administered to the experimental group, the only difference between the two groups was genetic factors. There were already significant differences in the biological processes related to lipid and glycometabolism, indicating that *ApoE* gene knockout greatly affects the lipid transport in mice in the experimental group, which is reflected by the urinary proteome very early. Acute phase reactions, immune responses, cytokines and proteolysis are also closely related to atherosclerosis [45-48].

(2) Urinary proteome changes during whole process

The literature shows that during the early stages of atherosclerosis, low-density lipoprotein (LDL) particles accumulate in the arterial intima, thereby being protected from plasma antioxidants, undergoing oxidation and other modifications and having proinflammatory and immunogenic properties. Classic monocytes circulating in the blood can exhibit anti-inflammatory functions and bind to the adhesion molecules expressed by activated endothelial cells to enter the inner membrane. Once in the inner membrane, monocytes can mature into macrophages, which express scavenger receptors that bind to lipoprotein particles and then become foam cells, finally forming the core of atherosclerotic plaques. T lymphocytes can also enter the inner membrane to regulate the functions of natural immune cells, endothelial cells and smooth muscle cells. The smooth muscle cells in the media can migrate to the inner membrane under the action of leukocytes to secrete extracellular matrix and form a fibrous cap [49]. During the exploration of this experiment, at week 1, the differentially expressed proteins between the experimental and control groups were related to the differentiation of epithelial cells, and cell adhesion was enriched in M1 macrophages, which may be related to the adhesion of monocytes. Differential proteins between the experimental and control groups at M2 were related to biological processes related to redox, which may be related to the redox of LDL particles. Cell adhesion also changes at M3, which may involve the recruitment of phagocytes. Numerous immune-related biological processes changed in M4, indicating the participation of immune cells, such as T cells. The regulation of fibroblast proliferation may be

related to the formation of fibrous caps. Enriched results revealed that proteolysis changed significantly at M5. It has been reported that activated macrophages can secrete proteolytic enzymes and degrade matrix components. The loss of matrix components may subsequently lead to plaque instability and increase the risk of plaque rupture and thrombosis [50]. Fibrin dissolution also plays an important role in the development of atherosclerosis [51].

The biological processes of the enrichment of differential proteins at different time points can correspond to the occurrence and development of atherosclerosis, indicating that the urinary proteome has the potential to be used to monitor the disease process.

After a week of a high-fat diet in the experimental group, the protein kinase B signalling pathway changed. It is reported to play an important role in the survival, proliferation and migration of macrophages and may affect the development of atherosclerosis [52]. After a month of a high-fat diet, many biological processes underwent significant changes. Studies have shown that urinary sodium excretion is the decisive factor of carotid intima-media thickness, which is an indicator of atherosclerosis [53]. The classical pathway of complement activation is also related to atherosclerosis [54]. Copper and isotype cysteine can interact to generate free radicals, thereby oxidizing LDL, which has been found in atherosclerotic plaques [55]. At M2, oestrogen has been reported to have a variety of anti-atherosclerotic properties, including affecting plasma lipoprotein levels and stimulating the production of prostacyclin and nitric oxide [56]. At M3, wound healing is also associated with atherosclerosis [40]. For the biological processes changed at M4, the ERK1/ERK2 pathway plays an important role in the proliferation of vascular smooth muscle cells induced by insulin (INS) and thrombin [43]. Alternative pathways of complement activation and major histocompatibility complex family II have been reported to be associated with atherosclerosis [57, 58]. In the enrichment of differential proteins at M5, chaperone-mediated autophagy (CMA) plays an important upstream regulatory role in lipid metabolism and lipid metabolism in liver cells [59].

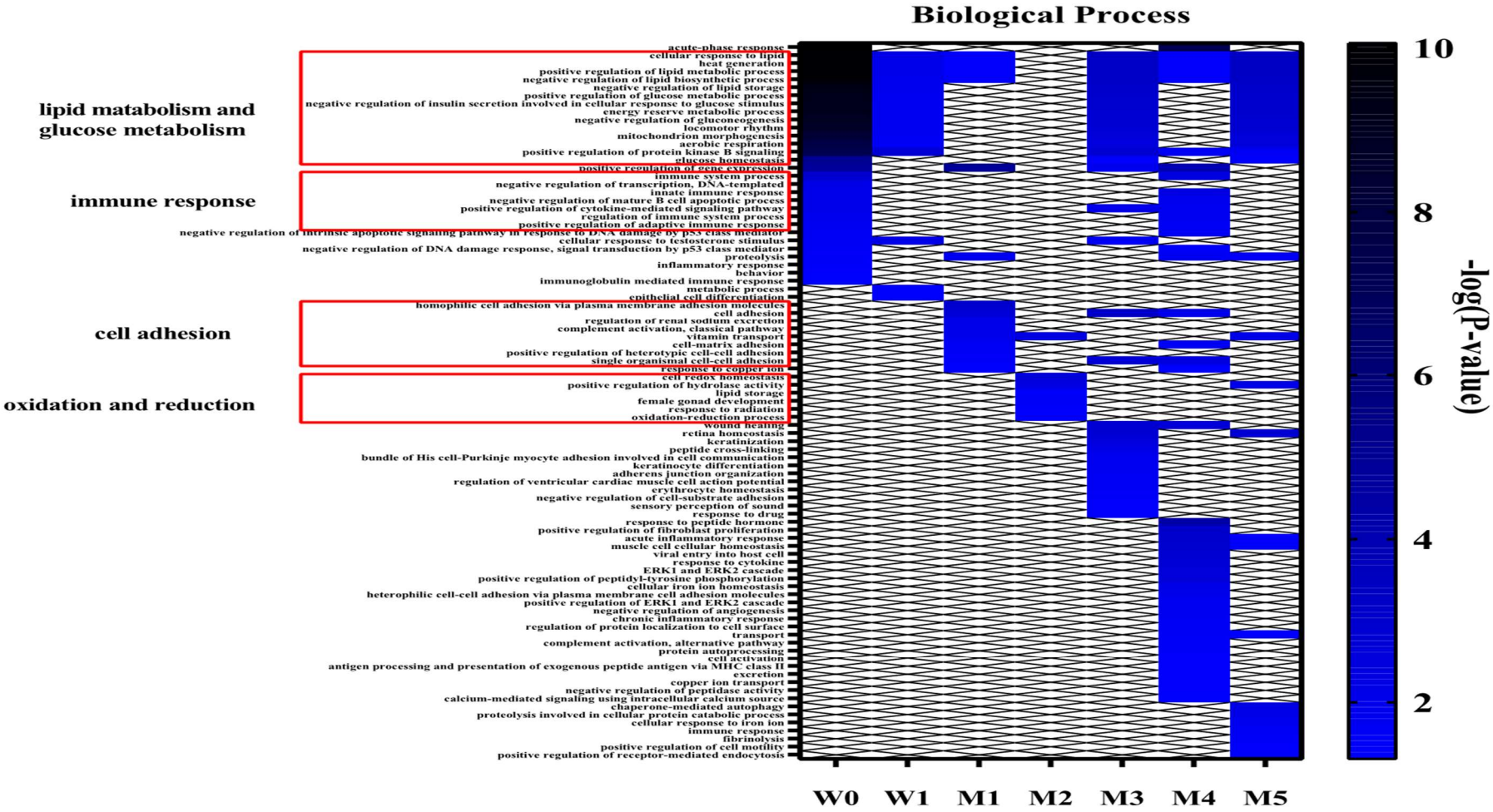

Figure 5 Functional annotation of differential proteins at different time points between the experimental and control groups (p <0.05)

When the experimental group was compared to the control group, there was a large difference in W0, demonstrating that the urinary proteome reflects even slight difference between the groups. In the subsequent control results at each time point, the degree of overlap in the differential proteins was small, but they were mostly related to lipids and cardiovascular diseases. The enriched biological processes also correspond to the progression of atherosclerosis, indicating that the urinary proteome is useful to monitor the disease process. However, as mentioned before, this type of comparison does not take the influence of diet and other factors into account.

3.3 Chemical modifications of proteins

To further explore the effect of high-fat diet on chemical modifications of urine proteins, a total of 15 samples were selected at three time points (EW0/EM5/CM5). After data retrieval (.raw) based on open-pFind software, the analysis results were exported in pBuild.

A total of 923 different chemical modification types were identified in 15 samples, of which 468 chemical modification types were identified in the EW0 group, 748 chemical modification types were identified in the EM5 group, and 611 chemical modification types were identified in the CM5 group.

a

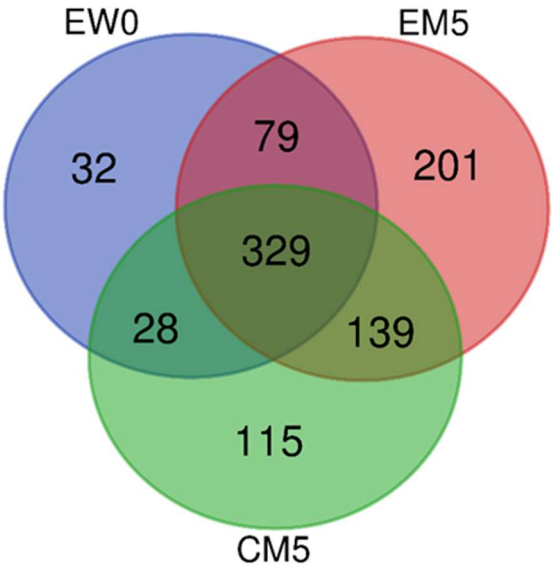

b

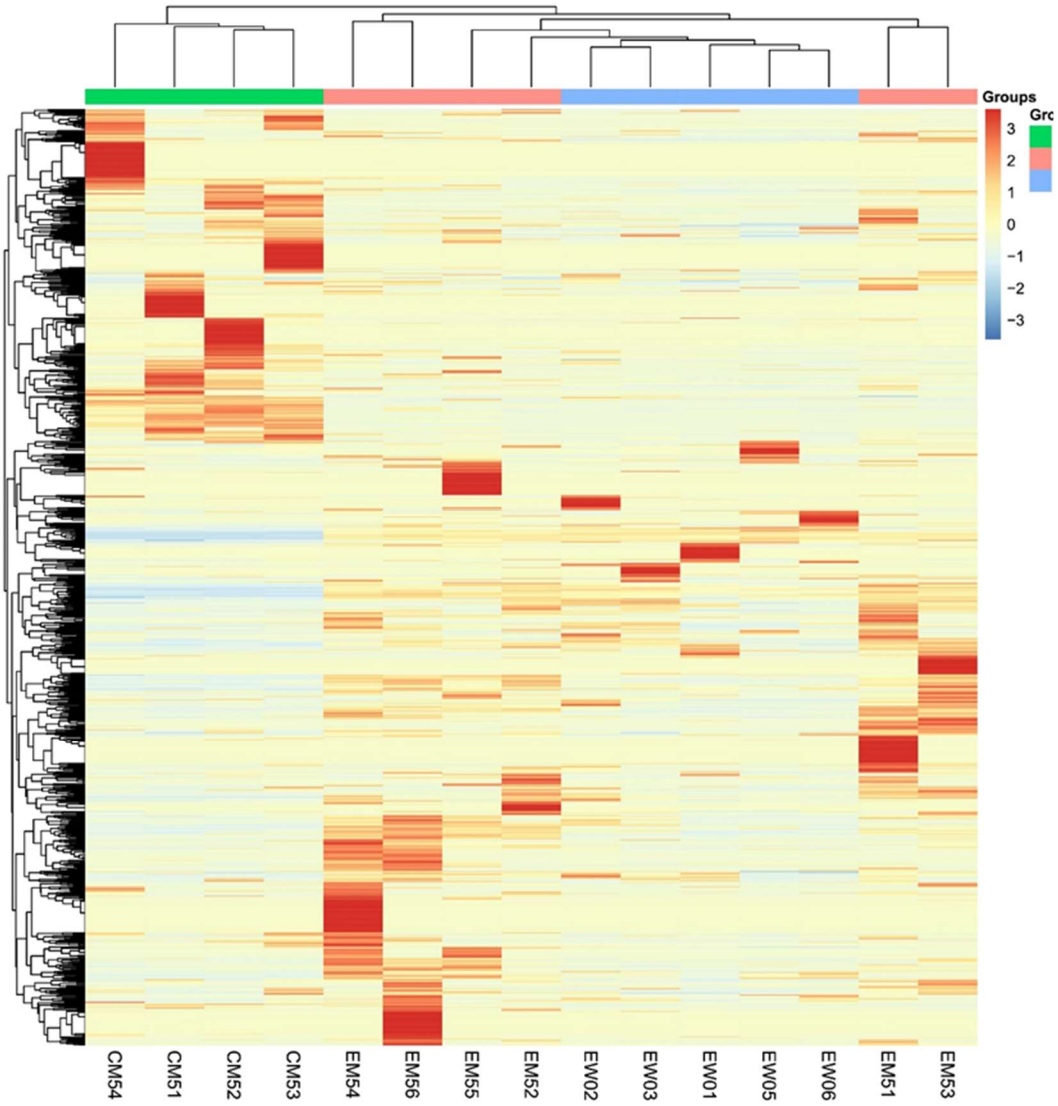

Figure 6 Chemical modifications among the three groups.

(a) Venn diagram of modification types among the three groups. (b) Unsupervised clustering of all the modification types in the three groups.

An unsupervised cluster analysis of all modifications found that the CM5 group was well distinguished from the other two groups (Figure 6). The percentages of different modification types in the EW0 group and the EM5 group were quantified to identify the modification changes that occurred in the internal controls. Among them, one modification type was unique to the EW0 group and existed in more than 4 samples (the total number of samples was 5), 23 modification types were unique to the EM5 group and existed in more than 5 samples (the total number of samples was 6), there are 68 types of modifications shared by the two groups, and there were significant differences (FC≥1.5 or ≤0.67, p <0.05). At the same time, the proportions of different types of modified sites in the CM5 group and the EM5 group were quantified, and the difference between the experimental group and the control group was analysed. Among them, 8 modification types were unique to the CM5 group and existed in more than 3 samples (the total number of samples was 4), and 19

371 modification types were unique to the EM5 group and existed in more than 5 samples (the total
372 number of samples was 6). There were 72 types of modifications that were shared by the two groups,
373 and there were significant differences (FC≥1.5 or ≤0.67, p <0.05) (see Table S5 for details).
374
375 To reduce the false negative influence caused by the open search mode, a restricted search
376 method was used for verification. Modification types that accounted for the top five modification
377 sites in the open search were fixed, modification types that were unique in a group and existed in
378 each sample and modification types that have been reported related to lipids in the literature are
379 selected. Twenty modifications in the EM5-EW0 group and 25 modifications in the EW5-CM5
380 group were selected, and the proportion of modified sites in the total number of sites was calculated
381 (Table S6). The screening criteria were FC≥1.5 or ≤ 0.67 and p <0.05. Finally, in the internal control
382 of the experimental group (EM5-EW0), the N-terminal carbamylation (Carbamyl[AnyN-term]), the
383 CHDH modification of aspartic acid (CHDH[D]), the tryptophan by kynurenine acid substitution
384 (Trp->Kynurenin[W]), oxidation modification of proline (Oxidation[P]), cysteine modification of
385 cysteine (Cysteinyl[C]), sulfur dioxide modification of cysteine (SulfurDioxide[C]), the
386 NO_SMX_SIMD modification of cysteine (NO_SMX_SIMD[C]) and the Delta_H(2)C(3)
387 modification of lysine (Delta_H(2)C(3)[K]) significantly changed. In the comparison between the
388 experimental and control groups (EM5-CM5), the guanidine modification of lysine (Guanidinyl[K]),
389 the phosphouridine modification of tyrosine (PhosphoUridine[Y]), the N-terminal carbamoyl
390 Modification (Carbamyl[AnyN-term]), Delta_H(2)C(2) modification (Delta_H(2)C(2)[AnyN-
391 term]) at the N-terminus and Dihydroxyimidazolidine modification of arginine
392 (Dihydroxyimidazolidine) [R]) showed significant changes.

UniProt	Human UniProt	Protein Name	P-value	Fold Change	References
B5X0G2	No	Major urinary protein 17	0.0008	7.92	[18]
P11588	No	Major urinary protein 1	0.0007	7.84	[18]
A2BIM8	No	Major urinary protein 18	0.0014	3.19	[18]
Q9JI02	No	Secretoglobin family 2B member 20	0.0488	2.75	—
Q5FW60	No	Major urinary protein 20	0.0121	2.65	[18]
Q07797	Q08380	Galectin-3-binding protein	0.0077	2.59	[60, 61]
Q61838	No	Pregnancy zone protein	0.0411	2.46	[62]
P11591	No	Major urinary protein 5	0.0136	2.40	[18]
Q64695	Q9UNN8	Endothelial protein C receptor	0.0150	2.23	[63]
Q91WR8	P59796	Glutathione peroxidase 6	0.0469	1.99	[64]
P06797	P07711	Cathepsin L1	0.0146	1.84	[65]
P13597	P05362	Intercellular adhesion molecule 1	0.0432	1.66	[66, 67]
Q9JK39	A8MVZ5	Butyrophilin-like protein 10	0.0446	0.60	—
P01898	P01891	H-2 class I histocompatibility antigen, Q10 alpha chain	0.0429	0.59	[68]
P55292	Q02487	Desmocollin-2	0.0160	0.57	[69, 70]
P23780	P16278	Beta-galactosidase	0.0384	0.56	—
Q60648	P17900	Ganglioside GM2 activator	0.0382	0.56	[71]
P00688	P04746	Pancreatic alpha-amylase	0.0311	0.55	[72]
P70269	P14091	Cathepsin E	0.0299	0.54	[73]
P11859	P01019	Angiotensinogen	0.0338	0.51	[20]
Q6UGQ3	No	Secretoglobin family 2B member 2	0.0270	0.49	—
O88322	Q14112	Nidogen-2	0.0004	0.43	—
O88968	P20062	Transcobalamin-2	0.0155	0.39	[23]
P11087	P02452	Collagen alpha-1(I) chain	0.0080	0.34	[21]

Q4KML4	Q9P1F3	Costars family protein ABRACL	0.0181	0.28	—
P35230	Q06141	Regenerating islet-derived protein 3-beta	0.0012	0.24	[24]
A2AEP0	No	Odorant-binding protein 1b	0.0213	0.20	[74]

Table 1 Details of differential proteins between week 1 and week 0 samples in the experimental group.

UniProt	Human UniProt	Protein Name	Fold Change							References
			EW0-CW0	EW1-CW1	EM1-CM1	EM2-CM2	EM3-CM3	EM4-CM4	EM5-CM5	
P35230	Q06141	Regenerating islet-derived protein 3-beta	5.22	—	—	—	—	—	—	[24]
P13020	P06396	Gelsolin	2.83	—	—	—	—	—	—	[26]
P97426	P12724	Eosinophil cationic protein 1	2.57	—	—	—	1.77	7.57	—	[75]
O88322	Q14112	Nidogen-2	2.32	1.96	—	—	—	—	0.39	—
P29699	P02765	Alpha-2-HS-glycoprotein	2.27	—	—	—	—	—	—	[25]
P07758	P01009	Alpha-1-antitrypsin 1-1	2.11	—	—	—	0.58	0.25	—	[21]
P07309	P02766	Transthyretin	2.06	—	—	—	—	—	—	[76]
P49183	P24855	Deoxyribonuclease-1	1.79	—	0.47	—	—	—	—	[77]
P01864	No	Ig gamma-2A chain C region secreted form	1.55	—	0.30	—	—	—	—	—
P19221	P00734	Prothrombin	0.63	—	—	—	—	—	0.54	[78]
P61110	P61109	Kidney androgen-regulated protein	0.62	—	—	—	—	6.55	—	[21]
Q9Z0M9	O95998	Interleukin-18-binding protein	0.60	—	—	—	2.11	—	—	[30]
P05533	No	Lymphocyte antigen 6A-2/6E-1	0.60	—	—	—	—	—	—	—
O09043	O96009	Napsin-A	0.59	—	—	—	0.42	—	—	—
P03953	P00746	Complement factor D	0.59	—	—	—	—	2.60	—	[79]
Q91VW3	Q9H299	SH3 domain-binding glutamic acid-rich-like protein 3	0.58	—	—	2.22	—	—	—	—
P15379	P16070	CD44 antigen	0.58	—	0.25	—	—	3.43	—	[80]
P04441	P04233	H-2 class II histocompatibility antigen gamma chain	0.54	—	—	—	4.59	13.02	—	[29]
P25119	P20333	Tumour necrosis factor receptor superfamily member 1B	0.54	—	—	—	1.74	—	—	[81]
Q00993	P30530	Tyrosine-protein kinase receptor UFO	0.53	—	—	0.51	2.16	3.62	—	[82]
P07361	P02763	Alpha-1-acid glycoprotein 2	0.52	—	—	—	—	0.13	—	[83]
P09470	P12821	Angiotensin-converting enzyme	0.51	—	—	—	—	—	—	[84]

Q91WR8	P59796	Glutathione peroxidase 6	0.47	—	—	—	—	3.34	—	[64]
Q62395	Q07654	Trefoil factor 3	0.46	—	—	—	—	—	—	[19]
Q9DAK9	Q9NRX4	14 kDa phosphohistidine phosphatase	0.46	—	—	—	—	—	2.02	[85]
O88188	O95711	Lymphocyte antigen 86	0.45	—	—	—	—	—	—	—
Q60932	P21796	Voltage-dependent anion-selective channel protein 1	0.44	0.45	—	3.68	—	—	—	[86]
P11589	No	Major urinary protein 2	0.44	—	3.82	—	1.98	6.19	3.16	[18]
Q62266	No	Cornifin-A	0.43	0.49	—	—	—	—	—	—
P17047	P13473	Lysosome-associated membrane glycoprotein 2	0.42	—	—	—	2.19	3.45	2.44	[31]
P0CW03	No	Lymphocyte antigen 6C2	0.41	—	—	—	—	—	—	—
Q60590	P02763	Alpha-1-acid glycoprotein 1	0.41	—	—	—	—	0.08	—	[83]
P01665	No	Ig kappa chain V-III region PC 7043	0.41	—	—	—	—	7.91	2.38	—
P04939	No	Major urinary protein 3	0.39	—	—	—	—	—	—	[18]
Q6SJQ5	Q6UXZ3	CMRF35-like molecule 3	0.35	—	—	—	—	—	0.56	—
Q64695	Q9UNN8	Endothelial protein C receptor	0.31	—	—	—	—	—	—	[63]
E9Q557	P15924	Desmoplakin	0.29	—	—	—	3.82	—	—	—
P11591	No	Major urinary protein 5	0.27	—	—	—	—	4.49	2.30	[18]
P51437	P49913	Cathelicidin antimicrobial peptide	0.24	—	—	—	—	—	—	[87]
Q5FW60	No	Major urinary protein 20	0.23	—	—	—	—	—	2.14	[18]
A2BIM8	No	Major urinary protein 18	0.20	0.50	6.10	—	2.10	—	—	[18]
Q61646	P00738	Haptoglobin	0.14	—	—	—	—	0.09	—	[28]
P11588	No	Major urinary protein 1	0.07	0.45	—	—	2.17	—	—	[18]
B5X0G2	No	Major urinary protein 17	0.06	0.34	28.79	—	—	—	4.06	[18]
Q9JI02	No	Secretoglobin family 2B member 20	—	2.83	—	—	0.23	—	—	—
Q01279	P00533	Epidermal growth factor receptor	—	1.52	—	—	—	—	—	[88]
P10605	P07858	Cathepsin B	—	0.63	0.44	—	—	—	—	[89]
P50429	P15848	Arylsulfatase B	—	0.56	—	—	—	—	—	[90]

Q571E4	P34059	N-acetylgalactosamine-6-sulfatase	—	0.52	—	—	—	3.57	—	—
Q9JK39	A8MVZ5	Butyrophilin-like protein 10	—	0.50	—	—	—	—	—	—
P23780	P16278	Beta-galactosidase	—	0.48	0.15	—	0.28	—	—	—
P70269	P14091	Cathepsin E	—	0.42	—	—	—	2.14	—	[73]
O35887	O43852	Calumenin	—	0.40	—	—	2.88	4.38	1.88	[91]
Q9EP95	Q9BQ08	Resistin-like alpha	—	0.27	—	—	—	—	0.20	[92]
P20152	P08670	Vimentin	—	—	16.24	—	—	—	—	[93]
Q8K0E8	P02675	Fibrinogen beta chain	—	—	8.28	—	—	—	—	[94]
P16858	P04406	Glyceraldehyde-3-phosphate dehydrogenase	—	—	4.72	—	—	—	—	[95]
Q9WTR5	P55290	Cadherin-13	—	—	2.78	—	—	—	—	[32]
Q00897	P01009	Alpha-1-antitrypsin 1-4	—	—	2.57	—	—	—	3.27	[21]
O09164	P08294	Extracellular superoxide dismutase [Cu-Zn]	—	—	2.11	1.56	—	3.37	—	[96]
P11276	P02751	Fibronectin	—	—	0.58	—	—	2.15	—	[33]
Q9Z0J0	P61916	NPC intracellular cholesterol transporter 2	—	—	0.57	—	—	—	—	[97]
Q8BPB5	Q12805	EGF-containing fibulin-like extracellular matrix protein 1	—	—	0.53	0.46	—	—	—	—
Q8BZT5	Q9H756	Leucine-rich repeat-containing protein 19	—	—	0.52	0.50	0.55	—	—	[98]
P21614	P02774	Vitamin D-binding protein	—	—	0.50	—	—	—	0.49	[99]
P16675	P10619	Lysosomal protective protein	—	—	0.49	—	—	—	2.51	—
Q61147	P00450	Ceruloplasmin	—	—	0.49	—	—	0.35	—	[100]
P23953	No	Carboxylesterase 1C	—	—	0.48	—	—	—	—	—
Q61398	Q15113	Procollagen C-endopeptidase enhancer 1	—	—	0.48	—	—	—	—	[101]
O35664	P48551	Interferon alpha/beta receptor 2	—	—	0.47	—	—	—	—	[102]
P11859	P01019	Angiotensinogen	—	—	0.45	—	—	0.15	—	[20]
P01898	P01891	H-2 class I histocompatibility antigen, Q10 alpha chain	—	—	0.45	—	—	—	2.03	[68]
C0HKG5	No	Ribonuclease T2-A	—	—	0.42	0.60	—	—	—	—
Q61271	P36896	Activin receptor type-1B	—	—	0.42	—	—	3.64	—	—

O88968	P20062	Transcobalamin-2	—	—	0.40	—	—	—	—	[23]
Q9Z0L8	Q92820	Gamma-glutamyl hydrolase	—	—	0.39	—	—	—	—	[103, 104]
P35459	Q14210	Lymphocyte antigen 6D	—	—	0.39	0.57	—	—	—	—
Q61129	P05156	Complement factor I	—	—	0.38	—	—	—	—	—
P01878	No	Ig alpha chain C region	—	—	0.38	—	5.03	—	—	—
P55292	Q02487	Desmocollin-2	—	—	0.38	—	3.72	—	—	[69, 70]
Q9JJS0	Q9NQ36	Signal peptide, CUB and EGF-like domain-containing protein 2	—	—	0.35	—	—	—	—	[27]
Q9Z319	Q9Y5Q5	Atrial natriuretic peptide-converting enzyme	—	—	0.35	—	—	—	—	[105]
P09036	P00995	Serine protease inhibitor Kazal-type 1	—	—	0.34	—	—	—	—	—
Q4KML4	Q9P1F3	Costars family protein ABRACL	—	—	0.33	—	2.18	—	—	—
Q925F2	Q96AP7	Endothelial cell-selective adhesion molecule	—	—	0.32	—	—	—	0.48	[106]
O89020	P43652	Afamin	—	—	0.31	0.50	—	—	—	[107]
Q9DAU7	Q14508	WAP four-disulfide core domain protein 2	—	—	0.31	—	—	—	—	—
Q8BND5	O00391	Sulfhydryl oxidase 1	—	—	0.30	0.40	—	—	0.61	—
P09803	P12830	Cadherin-1	—	—	0.29	—	2.78	2.34	—	[28]
P02816	P12273	Prolactin-inducible protein homolog	—	—	0.27	—	0.45	—	—	[37]
Q91WR6	Q9NU53	Glycoprotein integral membrane protein 1	—	—	0.26	0.59	—	—	0.45	—
Q3UDR8	Q9GZM5	Protein YIPF3	—	—	0.26	—	—	—	—	—
Q6UGQ3	No	Secretoglobin family 2B member 2	—	—	0.25	—	—	—	2.03	—
Q9D3H2	No	Odorant-binding protein 1a	—	—	0.25	—	1.75	—	—	[74]
P20060	P07686	Beta-hexosaminidase subunit beta	—	—	0.23	—	0.35	—	—	—
Q8K1H9	Q9NY56	Odorant-binding protein 2a	—	—	0.21	—	0.31	0.21	—	[74]
A2AEP0	No	Odorant-binding protein 1b	—	—	0.20	—	—	—	—	[74]
Q8C6C9	Q6P5S2	Protein LEG1 homolog	—	—	0.15	—	0.44	—	—	—
P00688	P04746	Pancreatic alpha-amylase	—	—	0.14	—	—	0.32	—	[72]

P10287	P22223	Cadherin-3	—	—	0.13	—	3.19	5.62	—	[28]
P56386	P60022	Beta-defensin 1	—	—	—	3.94	—	5.25	1.90	[108]
P10639	P10599	Thioredoxin	—	—	—	3.63	—	—	—	[109]
O88844	O75874	Isocitrate dehydrogenase [NADP] cytoplasmic	—	—	—	2.71	—	—	—	[110]
Q00623	P02647	Apolipoprotein A-I	—	—	—	2.07	—	—	0.36	[111]
P0CG49	P0CG47	Polyubiquitin-B	—	—	—	1.98	—	—	—	[112]
Q03404	Q03403	Trefoil factor 2	—	—	—	1.69	2.11	8.94	—	[19]
P15947	P06870	Kallikrein-1	—	—	—	0.66	—	1.74	—	[113]
O55186	P13987	CD59A glycoprotein	—	—	—	0.61	—	2.53	—	[114]
Q921I1	P02787	Serotransferrin	—	—	—	0.57	0.43	0.09	0.21	[35]
Q60648	P17900	Ganglioside GM2 activator	—	—	—	0.51	—	—	2.27	[72]
O88792	Q9Y624	Junctional adhesion molecule A	—	—	—	0.49	—	—	—	[115]
P07724	P02768	Albumin	—	—	—	0.38	—	0.38	0.43	[116]
O70554	No	Small proline-rich protein 2B	—	—	—	—	7.98	—	3.26	[117, 118]
Q62267	No	Cornifin-B	—	—	—	—	5.69	—	—	—
P35700	Q06830	Peroxiredoxin-1	—	—	—	—	3.75	—	—	[119]
P18761	P23280	Carbonic anhydrase 6	—	—	—	—	3.37	—	—	[120]
P01631	No	Ig kappa chain V-II region 26-10	—	—	—	—	3.29	3.00	—	—
P11087	P02452	Collagen alpha-1(I) chain	—	—	—	—	3.21	—	—	[21]
P01837	P01834	Immunoglobulin kappa constant	—	—	—	—	3.19	—	—	—
Q99N23	No	Carbonic anhydrase 15	—	—	—	—	2.91	—	—	[120]
P10126	P68104	Elongation factor 1-alpha 1	—	—	—	—	2.90	—	—	[121]
P70663	Q14515	SPARC-like protein 1	—	—	—	—	2.74	—	—	—
Q60847	Q99715	Collagen alpha-1(XII) chain	—	—	—	—	2.68	—	—	[21]
P29533	P19320	Vascular cell adhesion protein 1	—	—	—	—	2.62	2.12	—	[122]
O55135	P56537	Eukaryotic translation initiation factor 6	—	—	—	—	2.55	—	—	—

O54775	O95388	CCN family member 4	—	—	—	—	2.47	—	0.47	[22]
P01843	No	Ig lambda-1 chain C region	—	—	—	—	2.45	—	—	—
Q9DBV4	Q9BRK3	Matrix remodeling-associated protein 8	—	—	—	—	1.70	—	1.80	—
O35608	O15123	Angiopoietin-2	—	—	—	—	1.61	—	—	[123]
Q07797	Q08380	Galectin-3-binding protein	—	—	—	—	1.59	—	—	[60]
Q04519	P17405	Sphingomyelin phosphodiesterase	—	—	—	—	0.57	—	1.89	[124]
Q61838	No	Pregnancy zone protein	—	—	—	—	0.52	—	—	[62]
Q08423	P04155	Trefoil factor 1	—	—	—	—	—	12.79	—	[19]
O08997	O00244	Copper transport protein ATOX1	—	—	—	—	—	8.07	—	[125]
P03977	No	Ig kappa chain V-III region 50S10.1	—	—	—	—	—	4.79	—	—
P42567	P42566	Epidermal growth factor receptor substrate 15	—	—	—	—	—	4.53	—	[88]
Q91X17	P07911	Uromodulin	—	—	—	—	—	4.22	—	[126]
P57096	O43653	Prostate stem cell antigen	—	—	—	—	—	3.53	—	—
P70699	P10253	Lysosomal alpha-glucosidase	—	—	—	—	—	3.37	—	[127]
P01132	P01133	Pro-epidermal growth factor	—	—	—	—	—	3.13	—	—
P32507	Q92692	Nectin-2	—	—	—	—	—	3.03	—	[128]
Q5SSE9	Q86UQ4	ATP-binding cassette sub-family A member 13	—	—	—	—	—	2.92	—	—
P06797	O60911	Cathepsin L1	—	—	—	—	—	2.63	—	[65, 73]
Q8R242	Q01459	Di-N-acetylchitobiase	—	—	—	—	—	2.47	—	—
Q9Z0K8	O95497	Pantetheinase	—	—	—	—	—	2.32	3.65	—
O54782	Q9Y2E5	Epididymis-specific alpha-mannosidase	—	—	—	—	—	1.99	—	—
P22599	P01009	Alpha-1-antitrypsin 1-2	—	—	—	—	—	0.50	—	[21]
P13634	P00915	Carbonic anhydrase 1	—	—	—	—	—	0.39	3.37	[120]
P20918	P00747	Plasminogen	—	—	—	—	—	0.32	0.63	[129]
P07759	P01011	Serine protease inhibitor A3K	—	—	—	—	—	0.26	—	[36]
P02088	P68871	Hemoglobin subunit beta-1	—	—	—	—	—	0.24	—	—

P01027	P01024	Complement C3	—	—	—	—	—	0.20	—	[54]
Q00898	P01009	Alpha-1-antitrypsin 1-5	—	—	—	—	—	0.18	—	[21]
P11672	P80188	Neutrophil gelatinase-associated lipocalin	—	—	—	—	—	0.04	—	[130]
P01887	P61769	Beta-2-microglobulin	—	—	—	—	—	—	3.07	[131]
O09114	P41222	Prostaglandin-H2 D-isomerase	—	—	—	—	—	—	2.41	[132]
Q9WUU7	Q9UBR2	Cathepsin Z	—	—	—	—	—	—	2.32	[133]
Q8BHC0	Q9Y5Y7	Lymphatic vessel endothelial hyaluronic acid receptor 1	—	—	—	—	—	—	0.61	—
O70570	P01833	Polymeric immunoglobulin receptor	—	—	—	—	—	—	0.55	—
P26041	P26038	Moesin	—	—	—	—	—	—	0.53	[134]
Q7TMJ8	Q96FE7	Phosphoinositide-3-kinase-interacting protein 1	—	—	—	—	—	—	0.52	[135]
P01660	No	Ig kappa chain V-III region PC 3741/TEPC 111	—	—	—	—	—	—	0.43	—
Q60928	P19440	Glutathione hydrolase 1 proenzyme	—	—	—	—	—	—	0.39	[104]
P61971	P61970	Nuclear transport factor 2	—	—	—	—	—	—	0.36	—
P06330	No	Ig heavy chain V region AC38 205.12	—	—	—	—	—	—	0.36	—
Q921W8	Q8WVN6	Secreted and transmembrane protein 1A	—	—	—	—	—	—	0.35	—
Q8BX43	Q969Z4	Tumour necrosis factor receptor superfamily member 19L	—	—	—	—	—	—	0.33	[81]
Q9JM99	Q92954	Proteoglycan 4	—	—	—	—	—	—	0.26	[135]

398

399 Table 2 Details of differential proteins between the experimental group and the control group at different time points.

Among the changes observed in the internal control of the experimental group, many studies have shown that carbamylated proteins are involved in the occurrence of diseases, especially atherosclerosis and chronic renal failure [136]. The kynurenine pathway is the primary pathway of tryptophan metabolism and plays an important role in early atherosclerosis [137]. The oxidation of proline can form glutamate semialdehyde, and glutamate semialdehyde is closely related to lipid peroxidation[138]. Elevated plasma homocysteine has also been widely studied as an independent risk factor for atherosclerosis [139]. Obstruction of the sulfur dioxide/aspartate aminotransferase pathway is also known to be involved in the pathogenesis of many cardiovascular diseases [140]. The Delta_H(2)C(3) modification of lysine also refers to acrolein addition +38, and acrolein and other α- and β-unsaturated aldehydes are considered to be mediators of inflammation and vascular dysfunction [141]. CHDH modification of aspartic acid and NO_SMX_SIMD modification of cysteine have not been reported to be related to atherosclerosis and may act as potential modification sites.

Although it was not verified in a restricted search, there are also studies claiming that the interruption of cell signals mediated by electrophiles is related to the occurrence of atherosclerosis and cancer. HNE and ONE and their derivatives are both active lipid electrophile reagents that inhibit the release of proinflammatory factors to a certain extent [142]. Nε-carboxymethyl-lysine (CML) has been reported to accumulate in large amounts in the tissues of diabetes and atherosclerosis, and glucosone aldehyde is related to its formation [143]. Benzyl isothiocyanate salt has been reported to inhibit lipid production and fatty liver formation in obese mice fed a high-fat diet [144]. It has been reported in the literature that thiazolidine derivatives have a positive effect in the treatment of LDLR(-/-) atherosclerotic mice [145]. In addition, the carboxyethylation of lysine has also changed, and some literature indicates that the degree of carboxymethylation and carboxyethylation of lysine in the plasma of diabetic mice is significantly increased [146]. Changes in the expression of fucosylated oligosaccharides have been observed in pathological processes such as atherosclerosis [147]. In addition, the phosphorylation modification of tyrosine is related to the formation of esters, which may also be involved in lipid metabolism and the occurrence and progression of diseases.

In the differential modifications between the experimental group and the control group, some of the significantly changed modifications also changed in the internal control of the experimental group. In addition, the Delta_H(2)C(2) modification at the N-terminus of the amino acid also refers to acetaldehyde +26. In addition, acetaldehyde stimulates the growth of vascular smooth muscle cells in a notch-dependent manner, promoting the occurrence of atherosclerosis [148]. Advanced protein glycosylation is an important mechanism for the development of advanced complications of diabetes, including atherosclerosis. Hydroimidazolone-1 derived from methylglyoxal is the most abundant advanced glycosylation end product in human plasma [149]. In addition, the guanidine modification of lysine may also be related to atherosclerosis.

Although did not been verified in the restricted search, an increasing number of studies have shown that short-chain fatty acids and their homologous acylation are involved in cardiovascular disease, and the proportions of 2-hydroxyisobutyrylation, malonylation and crotonylation in the experimental group were significantly increased[150]. Nε-carboxymethyl-lysine (CML) has been reported to accumulate in large amounts in the tissues in diabetes and atherosclerosis, and its induced PI3K/Akt signal inhibition promotes foam cell apoptosis and the progression of atherosclerosis [151].

In addition, glucosone is closely related to its formation, the proportion of which also increased significantly in the experimental group. Oxidation of tyrosine produces dihydroxyphenylalanine (DOPA), and the protein binding DOPA in tissues is elevated in many age-related pathological diseases, such as atherosclerosis and cataract formation [152].

As mentioned above, the internal controls of the experimental group avoid the influence of genes, diet and other factors on the urinary proteome, but they may be affected by the growth and development of the organisms themselves. Intergroup control avoids the influence of development but cannot avoid factors such as diet. The identification results of chemical modifications of urine proteins showed that regardless of whether internal control or intergroup control was adopted, the modification status changed greatly and was closely related to lipids and cardiovascular diseases. In comparison, differences in the intergroup control may be more obvious.

4 Conclusion

This study explored changes in urinary proteomics of high-fat diet-fed *ApoE*$^{-/-}$ mice. The internal control results showed that even after only one week of a high-fat diet, when the urinary proteome of the control group was not significantly changed, the urinary proteome of the experimental group had changed significantly, and most of the enriched biological pathways were related to lipid metabolism and glycometabolism, indicating that the urinary proteome has the potential for early and sensitive monitoring of biological changes. Most of the proteins and their family members that change continually in disease progression have been reported to be related to cardiovascular diseases or can be used as biomarkers. The results of the intergroup comparison showed that the biological processes enriched by differential proteins at different time points correspond to the occurrence and development of the atherosclerosis, indicating that the urinary proteome has the potential to be used to monitor the disease process. The differential modification types in the internal control of the experimental group and the comparison between the experimental and control groups have also been reported to be related to lipids and cardiovascular diseases, which can be used as a reference for identifying new biomarkers.

Declaration

Ethics approval and consent to participate

All animal protocols governing the experiments in this study were approved by the Institute of Basic Medical Sciences Animal Ethics Committee, Peking Union Medical College (Approved ID: ACUC-A02-2014-007).

Consent for publication

Not applicable.

Availability of data and material

The mass spectrometry proteomics data have been deposited to the ProteomeXchange Consortium (http://proteomecentral.proteomexchange.org) via the iProX partner repository with the dataset identifier PXD027610.

Competing interests

The authors declare that they have no known competing financial interests or personal relationships that could have appeared to influence the work reported in this paper.

Funding

This work was supported by the National Key Research and Development Program of China (2018YFC0910202 and 2016YFC1306300); the Fundamental Research Funds for the Central Universities (2020KJZX002); the Beijing Natural Science Foundation (7172076); the Beijing Cooperative Construction Project (110651103); the Beijing Normal University (11100704); and the Peking Union Medical College Hospital (2016-2.27).

Authors' contributions

Hua Yuanrui performed the experiments, analyzed the data, contributed reagents/materials/ analysis tools, prepared figures and/or tables, authored or reviewed drafts of the paper, approved the final draft. **Meng Wenshu** and **Wei Jing** performed the experiments and contributed reagents/materials/analysis tools. **Liu Yongtao** analyzed the data and contributed reagents/materials/analysis tools. **Gao Youhe** conceived and designed the experiments, authored or reviewed drafts of the paper, approved the final draft.

Acknowledgements

Not applicable.

References

1. Rahman, M.S. and K. Woollard, *Atherosclerosis.* Adv Exp Med Biol, 2017. **1003**: p. 121-144.
2. Tabas, I., G. Garcia-Cardena, and G.K. Owens, *Recent insights into the cellular biology of atherosclerosis.* J Cell Biol, 2015. **209**(1): p. 13-22.
3. *World Health Organization. Cardiovascular diseases (CVDs) Fact Sheet.* 2017.
4. Gao, Y., *Urine-an untapped goldmine for biomarker discovery?* Sci China Life Sci, 2013. **56**(12): p. 1145-6.
5. Ni, Y., et al., *Early candidate biomarkers found from urine of glioblastoma multiforme rat before changes in MRI.* Sci China Life Sci, 2018. **61**(8): p. 982-987.
6. Wei, J., W. Meng, and Y. Gao, *Urine proteome changes in rats subcutaneously inoculated with approximately ten tumor cells.* PeerJ, 2019. **7**: p. e7717.
7. Zhao, M., et al., *Dynamic changes of urinary proteins in a focal segmental glomerulosclerosis rat model.* Proteome Sci, 2014. **12**: p. 42.
8. Hatters, D.M., C.A. Peters-Libeu, and K.H. Weisgraber, *Apolipoprotein E structure: insights into function.* Trends Biochem Sci, 2006. **31**(8): p. 445-54.
9. Rosenfeld, M.E., et al., *Advanced atherosclerotic lesions in the innominate artery of the ApoE knockout mouse.* Arterioscler Thromb Vasc Biol, 2000. **20**(12): p. 2587-92.
10. Qu, G., et al., *The promotion effect of novel magnetic nanoparticles on atherosclerotic plaque vulnerability in apolipoprotein E(-/-) mice.* Toxicology, 2019. **419**: p. 24-31.
11. Wisniewski, J.R., et al., *Universal sample preparation method for proteome analysis.* Nat Methods, 2009. **6**(5): p. 359-62.
12. Bruderer, R., et al., *Extending the limits of quantitative proteome profiling with data-independent acquisition and application to acetaminophen-treated three-dimensional liver microtissues.* Mol Cell Proteomics, 2015. **14**(5): p. 1400-10.
13. Chi, H., et al., *Comprehensive identification of peptides in tandem mass spectra using an efficient open search engine.* Nat Biotechnol, 2018.
14. Armitage, E.G., et al., *Missing value imputation strategies for metabolomics data.* Electrophoresis, 2015. **36**(24): p. 3050-60.
15. Wang, S., et al., *NAguideR: performing and prioritizing missing value imputations for consistent bottom-up proteomic analyses.* Nucleic Acids Res, 2020. **48**(14): p. e83.
16. Huang da, W., B.T. Sherman, and R.A. Lempicki, *Systematic and integrative analysis of large gene lists using DAVID bioinformatics resources.* Nat Protoc, 2009. **4**(1): p. 44-57.
17. Ma, J., et al., *iProX: an integrated proteome resource.* Nucleic Acids Res, 2019. **47**(D1): p. D1211-D1217.
18. Kwak, J., et al., *Are MUPs a Toxic Waste Disposal System?* PLoS One, 2016. **11**(3): p. e0151474.
19. De Giorgio, M.R., et al., *Trefoil factor family member 2 (Tff2) KO mice are protected from high-fat diet-induced obesity.* Obesity (Silver Spring), 2013. **21**(7): p. 1389-95.
20. Carroll, W.X., et al., *Angiotensinogen gene silencing reduces markers of lipid accumulation and inflammation in cultured adipocytes.* Front Endocrinol (Lausanne), 2013. **4**: p. 10.
21. von zur Muhlen, C., et al., *Urine proteome analysis reflects atherosclerotic disease in an*

ApoE-/- mouse model and allows the discovery of new candidate biomarkers in mouse and human atherosclerosis. Mol Cell Proteomics, 2012. **11**(7): p. M111 013847.

22. Liu, H., et al., *CCN4 regulates vascular smooth muscle cell migration and proliferation.* Mol Cells, 2013. **36**(2): p. 112-8.
23. Celik, S.F. and E. Celik, *Subclinical atherosclerosis and impaired cardiac autonomic control in pediatric patients with Vitamin B12 deficiency.* Niger J Clin Pract, 2018. **21**(8): p. 1012-1016.
24. K, M., et al., *Association of serum regenerating islet-derived protein 3-beta and oncostatin-M levels with the risk of acute coronary syndrome in patients with type 2 diabetes mellitus - A pilot study.* Diabetes Metab Syndr, 2020. **14**(5): p. 1087-1092.
25. Muendlein, A., et al., *Are AHSG polymorphisms directly associated with coronary atherosclerosis?* Clin Chim Acta, 2012. **413**(1-2): p. 287-90.
26. de la Cuesta, F., et al., *Deregulation of smooth muscle cell cytoskeleton within the human atherosclerotic coronary media layer.* J Proteomics, 2013. **82**: p. 155-65.
27. Ali, H., et al., *Localization and characterization of a novel secreted protein, SCUBE2, in the development and progression of atherosclerosis.* Kobe J Med Sci, 2013. **59**(4): p. E122-31.
28. Langlois, M.R. and J.R. Delanghe, *Biological and clinical significance of haptoglobin polymorphism in humans.* Clin Chem, 1996. **42**(10): p. 1589-600.
29. Wigren, M., et al., *Lack of Ability to Present Antigens on Major Histocompatibility Complex Class II Molecules Aggravates Atherosclerosis in ApoE(-/-) Mice.* Circulation, 2019. **139**(22): p. 2554-2566.
30. Dinarello, C.A., *Interleukin-18 and the pathogenesis of inflammatory diseases.* Semin Nephrol, 2007. **27**(1): p. 98-114.
31. Wu, G., et al., *LAMP-2 gene expression in peripheral leukocytes is increased in patients with coronary artery disease.* Clin Cardiol, 2011. **34**(4): p. 239-43.
32. Fujishima, Y., et al., *Adiponectin association with T-cadherin protects against neointima proliferation and atherosclerosis.* FASEB J, 2017. **31**(4): p. 1571-1583.
33. Stenman, S., K. von Smitten, and A. Vaheri, *Fibronectin and atherosclerosis.* Acta Med Scand Suppl, 1980. **642**: p. 165-70.
34. Ichiki, T., *Thyroid hormone and atherosclerosis.* Vascul Pharmacol, 2010. **52**(3-4): p. 151-6.
35. Kibel, A., T. Belovari, and I. Drenjancevic-Peric, *The role of transferrin in atherosclerosis.* Med Hypotheses, 2008. **70**(4): p. 793-7.
36. Wagsater, D., et al., *Serine protease inhibitor A3 in atherosclerosis and aneurysm disease.* Int J Mol Med, 2012. **30**(2): p. 288-94.
37. Sauro, M.D. and N.E. Zorn, *Prolactin induces proliferation of vascular smooth muscle cells through a protein kinase C-dependent mechanism.* J Cell Physiol, 1991. **148**(1): p. 133-8.
38. Hartman, J. and W.H. Frishman, *Inflammation and atherosclerosis: a review of the role of interleukin-6 in the development of atherosclerosis and the potential for targeted drug therapy.* Cardiol Rev, 2014. **22**(3): p. 147-51.
39. Tinajero, M.G. and A.I. Gotlieb, *Recent Developments in Vascular Adventitial Pathobiology: The Dynamic Adventitia as a Complex Regulator of Vascular Disease.* Am J Pathol, 2020. **190**(3): p. 520-534.
40. Natarelli, L. and A. Schober, *MicroRNAs and the response to injury in atherosclerosis.*

Hamostaseologie, 2015. **35**(2): p. 142-50.

41. Wight, T.N., *The extracellular matrix and atherosclerosis.* Curr Opin Lipidol, 1995. **6**(5): p. 326-34.
42. Fernandez-Murga, M.L., et al., *Impact of estrogens on atherosclerosis and bone in the apolipoprotein E-deficient mouse model.* Menopause, 2015. **22**(4): p. 428-36.
43. Isenovic, E.R., et al., *Insulin, thrombine, ERK1/2 kinase and vascular smooth muscle cells proliferation.* Curr Pharm Des, 2010. **16**(35): p. 3895-902.
44. Chi, Z. and A.J. Melendez, *Role of cell adhesion molecules and immune-cell migration in the initiation, onset and development of atherosclerosis.* Cell Adh Migr, 2007. **1**(4): p. 171-5.
45. Whicher, J., L. Biasucci, and N. Rifai, *Inflammation, the acute phase response and atherosclerosis.* Clin Chem Lab Med, 1999. **37**(5): p. 495-503.
46. van Dijk, R.A., et al., *Systematic Evaluation of the Cellular Innate Immune Response During the Process of Human Atherosclerosis.* J Am Heart Assoc, 2016. **5**(6).
47. Tedgui, A. and Z. Mallat, *Cytokines in atherosclerosis: pathogenic and regulatory pathways.* Physiol Rev, 2006. **86**(2): p. 515-81.
48. Garcia-Touchard, A., et al., *Extracellular proteases in atherosclerosis and restenosis.* Arterioscler Thromb Vasc Biol, 2005. **25**(6): p. 1119-27.
49. Libby, P., et al., *Atherosclerosis.* Nat Rev Dis Primers, 2019. **5**(1): p. 56.
50. Hansson, G.K., A.K. Robertson, and C. Soderberg-Naucler, *Inflammation and atherosclerosis.* Annu Rev Pathol, 2006. **1**: p. 297-329.
51. Sueishi, K., et al., *Atherosclerosis: coagulation and fibrinolysis.* Semin Thromb Hemost, 1998. **24**(3): p. 255-60.
52. Linton, M.F., J.J. Moslehi, and V.R. Babaev, *Akt Signaling in Macrophage Polarization, Survival, and Atherosclerosis.* Int J Mol Sci, 2019. **20**(11).
53. Ustundag, S., et al., *Carotid intima media thickness is independently associated with urinary sodium excretion in patients with chronic kidney disease.* Ren Fail, 2015. **37**(8): p. 1285-92.
54. Drapkina, O.M., B.B. Gegenava, and V.V. Fomin, *The role of the mLDL-induced activation of the complement system classical pathway and C3 expression stimulation in atherosclerosis.* Ter Arkh, 2018. **90**(4): p. 100-104.
55. Jomova, K. and M. Valko, *Advances in metal-induced oxidative stress and human disease.* Toxicology, 2011. **283**(2-3): p. 65-87.
56. Nathan, L. and G. Chaudhuri, *Estrogens and atherosclerosis.* Annu Rev Pharmacol Toxicol, 1997. **37**: p. 477-515.
57. Wunderer, F., et al., *The role of hepcidin and iron homeostasis in atherosclerosis.* Pharmacol Res, 2020. **153**: p. 104664.
58. Williams, J.W., et al., *B Cell-Mediated Antigen Presentation through MHC Class II Is Dispensable for Atherosclerosis Progression.* Immunohorizons, 2019. **3**(1): p. 37-44.
59. Qiao, L., et al., *Deficient Chaperone-Mediated Autophagy Promotes Lipid Accumulation in Macrophage.* J Cardiovasc Transl Res, 2020.
60. Sano, H., et al., *Human galectin-3 is a novel chemoattractant for monocytes and macrophages.* J Immunol, 2000. **165**(4): p. 2156-64.
61. Papaspyridonos, M., et al., *Galectin-3 is an amplifier of inflammation in atherosclerotic*

plaque progression through macrophage activation and monocyte chemoattraction. Arterioscler Thromb Vasc Biol, 2008. **28**(3): p. 433-40.

62. Sanchez, M.C., G.A. Chiabrando, and M.A. Vides, *Pregnancy zone protein-tissue-type plasminogen activator complexes bind to low-density lipoprotein receptor-related protein (LRP).* Arch Biochem Biophys, 2001. **389**(2): p. 218-22.
63. Navarro, S., et al., *The endothelial cell protein C receptor: its role in thrombosis.* Thromb Res, 2011. **128**(5): p. 410-6.
64. Lin, M.S., et al., *Higher glutathione peroxidase expression in thoracic aorta as a protective factor against oxidative stress and atherosclerosis in rabbits.* Cardiology, 2007. **108**(4): p. 381-6.
65. Li, W., et al., *Cathepsin L is significantly associated with apoptosis and plaque destabilization in human atherosclerosis.* Atherosclerosis, 2009. **202**(1): p. 92-102.
66. Ohta, T., et al., *Soluble vascular cell-adhesion molecule-1 and soluble intercellular adhesion molecule-1 correlate with lipid and apolipoprotein risk factors for coronary artery disease in children.* Eur J Pediatr, 1999. **158**(7): p. 592-8.
67. Li, X., R.F. Li, and S.W. Ding, *[Effect of xinhe granule on vascular endothelial damage and endothelial expressed endothelin and intercellular adhesion molecule-1 in rats fed with high lipid diet].* Zhongguo Zhong Xi Yi Jie He Za Zhi, 2001. **21**(8): p. 602-4.
68. Fortin, C.F., et al., *Aging and neutrophils: there is still much to do.* Rejuvenation Res, 2008. **11**(5): p. 873-82.
69. Li, Y.B., et al., *Oxidized low-density lipoprotein attenuated desmoglein 1 and desmocollin 2 expression via LOX-1/Ca(2+)/PKC-beta signal in human umbilical vein endothelial cells.* Biochem Biophys Res Commun, 2015. **468**(1-2): p. 380-6.
70. Jiang, K., et al., *Galectin-3 regulates desmoglein-2 and intestinal epithelial intercellular adhesion.* J Biol Chem, 2014. **289**(15): p. 10510-7.
71. Yanai, H., et al., *The possible contribution of a general glycosphingolipid transporter, GM2 activator protein, to atherosclerosis.* J Atheroscler Thromb, 2006. **13**(6): p. 281-5.
72. Ozkok, A., et al., *Low serum pancreatic enzyme levels predict mortality and are associated with malnutrition-inflammation-atherosclerosis syndrome in patients with chronic kidney disease.* Int Urol Nephrol, 2013. **45**(2): p. 477-84.
73. Kadowaki, T., et al., *Defective adipose tissue development associated with hepatomegaly in cathepsin E-deficient mice fed a high-fat diet.* Biochem Biophys Res Commun, 2014. **446**(1): p. 212-7.
74. Grolli, S., et al., *Odorant binding protein has the biochemical properties of a scavenger for 4-hydroxy-2-nonenal in mammalian nasal mucosa.* FEBS J, 2006. **273**(22): p. 5131-42.
75. Niccoli, G., et al., *Eosinophil cationic protein: A new biomarker of coronary atherosclerosis.* Atherosclerosis, 2010. **211**(2): p. 606-11.
76. Yang, C.S., et al., *Proteomic analysis of prognostic plasma biomarkers in peripheral arterial occlusive disease.* Mol Biosyst, 2017. **13**(7): p. 1297-1303.
77. Josefs, T., et al., *Neutrophil extracellular traps promote macrophage inflammation and impair atherosclerosis resolution in diabetic mice.* JCI Insight, 2020. **5**(7).
78. Posma, J.J., J.J. Posthuma, and H.M. Spronk, *Coagulation and non-coagulation effects of thrombin.* J Thromb Haemost, 2016. **14**(10): p. 1908-1916.
79. Shin, S.K., et al., *Long-term curcumin administration protects against atherosclerosis via*

hepatic regulation of lipoprotein cholesterol metabolism. Mol Nutr Food Res, 2011. **55**(12): p. 1829-40.

80. Krolikoski, M., J. Monslow, and E. Pure, *The CD44-HA axis and inflammation in atherosclerosis: A temporal perspective.* Matrix Biol, 2019. **78-79**: p. 201-218.
81. Smeets, E., S. Meiler, and E. Lutgens, *Lymphocytic tumor necrosis factor receptor superfamily co-stimulatory molecules in the pathogenesis of atherosclerosis.* Curr Opin Lipidol, 2013. **24**(6): p. 518-24.
82. van der Meer, J.H., T. van der Poll, and C. van 't Veer, *TAM receptors, Gas6, and protein S: roles in inflammation and hemostasis.* Blood, 2014. **123**(16): p. 2460-9.
83. Puerta, A., et al., *Study of the capillary electrophoresis profile of intact alpha-1-acid glycoprotein isoforms as a biomarker of atherothrombosis.* Analyst, 2011. **136**(4): p. 816-22.
84. Jiang, F., et al., *Angiotensin-converting enzyme 2 and angiotensin 1-7: novel therapeutic targets.* Nat Rev Cardiol, 2014. **11**(7): p. 413-26.
85. Wieland, T. and P.V. Attwood, *Alterations in reversible protein histidine phosphorylation as intracellular signals in cardiovascular disease.* Front Pharmacol, 2015. **6**: p. 173.
86. Chen, H., et al., *Inhibition of VDAC1 prevents Ca(2)(+)-mediated oxidative stress and apoptosis induced by 5-aminolevulinic acid mediated sonodynamic therapy in THP-1 macrophages.* Apoptosis, 2014. **19**(12): p. 1712-26.
87. Edfeldt, K., et al., *Involvement of the antimicrobial peptide LL-37 in human atherosclerosis.* Arterioscler Thromb Vasc Biol, 2006. **26**(7): p. 1551-7.
88. Wang, L., et al., *Inhibition of epidermal growth factor receptor attenuates atherosclerosis via decreasing inflammation and oxidative stress.* Sci Rep, 2017. **8**: p. 45917.
89. Zhao, C.F. and D.M. Herrington, *The function of cathepsins B, D, and X in atherosclerosis.* Am J Cardiovasc Dis, 2016. **6**(4): p. 163-170.
90. Biros, E., et al., *Upregulation of arylsulfatase B in carotid atherosclerosis is associated with symptoms of cerebral embolization.* Sci Rep, 2017. **7**(1): p. 4338.
91. Hernandez-Romero, D., et al., *CALU A29809G polymorphism in coronary atherothrombosis: Implications for coronary calcification and prognosis.* Ann Med, 2010. **42**(6): p. 439-46.
92. Asano, T., et al., *Physiological significance of resistin and resistin-like molecules in the inflammatory process and insulin resistance.* Curr Diabetes Rev, 2006. **2**(4): p. 449-54.
93. Haversen, L., et al., *Vimentin deficiency in macrophages induces increased oxidative stress and vascular inflammation but attenuates atherosclerosis in mice.* Sci Rep, 2018. **8**(1): p. 16973.
94. Oszajca, K., et al., *Association analysis of genetic polymorphisms of factor V, factor VII and fibrinogen beta chain genes with human abdominal aortic aneurysm.* Exp Ther Med, 2012. **4**(3): p. 514-518.
95. Li, Y.Q., et al., *Regulation of endothelial cell survival and death by the MAP kinase/ERK kinase kinase 3 - glyceraldehyde-3-phosphate dehydrogenase signaling axis.* Cell Signal, 2019. **58**: p. 20-33.
96. Fukai, T., et al., *Vascular expression of extracellular superoxide dismutase in atherosclerosis.* J Clin Invest, 1998. **101**(10): p. 2101-11.
97. Yu, X.H., et al., *NPC1, intracellular cholesterol trafficking and atherosclerosis.* Clin Chim

Acta, 2014. **429**: p. 69-75.

98. Sun, J., Z. Wang, and X. Wang, *Suppression of LRRC19 promotes cutaneous wound healing in pressure ulcers in mice.* Organogenesis, 2018. **14**(1): p. 13-24.
99. Gouni-Berthold, I., W. Krone, and H.K. Berthold, *Vitamin D and cardiovascular disease.* Curr Vasc Pharmacol, 2009. **7**(3): p. 414-22.
100. Arenas de Larriva, A.P., et al., *Circulating ceruloplasmin, ceruloplasmin-associated genes and the incidence of venous thromboembolism in the Atherosclerosis Risk in Communities study.* J Thromb Haemost, 2019. **17**(5): p. 818-826.
101. Pollard, R.D., et al., *Procollagen C-endopeptidase Enhancer Protein 2 (PCPE2) Reduces Atherosclerosis in Mice by Enhancing Scavenger Receptor Class B1 (SR-BI)-mediated High-density Lipoprotein (HDL)-Cholesteryl Ester Uptake.* J Biol Chem, 2015. **290**(25): p. 15496-511.
102. Teunissen, P.F., et al., *MAb therapy against the IFN-alpha/beta receptor subunit 1 stimulates arteriogenesis in a murine hindlimb ischaemia model without enhancing atherosclerotic burden.* Cardiovasc Res, 2015. **107**(2): p. 255-66.
103. Bachhawat, A.K. and S. Yadav, *The glutathione cycle: Glutathione metabolism beyond the gamma-glutamyl cycle.* IUBMB Life, 2018. **70**(7): p. 585-592.
104. Presnell, C.E., et al., *Computational insights into the role of glutathione in oxidative stress.* Curr Neurovasc Res, 2013. **10**(2): p. 185-94.
105. Ichiki, T., et al., *Endothelial permeability in vitro and in vivo: protective actions of ANP and omapatrilat in experimental atherosclerosis.* Peptides, 2013. **48**: p. 21-6.
106. Inoue, M., et al., *Endothelial cell-selective adhesion molecule modulates atherosclerosis through plaque angiogenesis and monocyte-endothelial interaction.* Microvasc Res, 2010. **80**(2): p. 179-87.
107. Franca, K.C., et al., *Quiescin/sulfhydryl oxidase 1b (QSOX1b) induces migration and proliferation of vascular smooth muscle cells by distinct redox pathways.* Arch Biochem Biophys, 2020. **679**: p. 108220.
108. Bian, T., et al., *Human beta-Defensin 3 Reduces TNF-alpha-Induced Inflammation and Monocyte Adhesion in Human Umbilical Vein Endothelial Cells.* Mediators Inflamm, 2017. **2017**: p. 8529542.
109. Couchie, D., et al., *Human Plasma Thioredoxin-80 Increases With Age and in ApoE(-/-) Mice Induces Inflammation, Angiogenesis, and Atherosclerosis.* Circulation, 2017. **136**(5): p. 464-475.
110. Fu, X., et al., *7-Ketocholesterol inhibits isocitrate dehydrogenase 2 expression and impairs endothelial function via microRNA-144.* Free Radic Biol Med, 2014. **71**: p. 1-15.
111. Smith, J.D., *Apolipoprotein A-I and its mimetics for the treatment of atherosclerosis.* Curr Opin Investig Drugs, 2010. **11**(9): p. 989-96.
112. Hewing, B., et al., *Immunoproteasome subunit ss5i/LMP7-deficiency in atherosclerosis.* Sci Rep, 2017. **7**(1): p. 13342.
113. Zhang, Y., et al., *Association of the KLK1 rs5516 G allele and the ACE D allele with aortic aneurysm and atherosclerotic stenosis.* Medicine (Baltimore), 2016. **95**(44): p. e5120.
114. Lewis, R.D., et al., *The membrane attack complex of complement drives the progression of atherosclerosis in apolipoprotein E knockout mice.* Mol Immunol, 2010. **47**(5): p. 1098-105.

115. Karshovska, E., et al., *Hyperreactivity of junctional adhesion molecule A-deficient platelets accelerates atherosclerosis in hyperlipidemic mice.* Circ Res, 2015. **116**(4): p. 587-99.
116. Allawi, A.A.D., *Malnutrition, inflamation and atherosclerosis (MIA syndrome) in patients with end stage renal disease on maintenance hemodialysis (a single centre experience).* Diabetes Metab Syndr, 2018. **12**(2): p. 91-97.
117. Segedy, A.K., et al., *Identification of small proline-rich repeat protein 3 as a novel atheroprotective factor that promotes adaptive Akt signaling in vascular smooth muscle cells.* Arterioscler Thromb Vasc Biol, 2014. **34**(12): p. 2527-36.
118. Burke, R.M., et al., *Small proline-rich protein 2B drives stress-dependent p53 degradation and fibroblast proliferation in heart failure.* Proc Natl Acad Sci U S A, 2018. **115**(15): p. E3436-E3445.
119. Madrigal-Matute, J., et al., *Thioredoxin-1/peroxiredoxin-1 as sensors of oxidative stress mediated by NADPH oxidase activity in atherosclerosis.* Free Radic Biol Med, 2015. **86**: p. 352-61.
120. Yuan, L., et al., *Carbonic Anhydrase 1-Mediated Calcification Is Associated With Atherosclerosis, and Methazolamide Alleviates Its Pathogenesis.* Front Pharmacol, 2019. **10**: p. 766.
121. Zhang, P., et al., *Impairing eukaryotic elongation factor 2 kinase activity decreases atherosclerotic plaque formation.* Can J Cardiol, 2014. **30**(12): p. 1684-8.
122. Habas, K. and L. Shang, *Alterations in intercellular adhesion molecule 1 (ICAM-1) and vascular cell adhesion molecule 1 (VCAM-1) in human endothelial cells.* Tissue Cell, 2018. **54**: p. 139-143.
123. Yu, H., et al., *Angiopoietin-2 attenuates angiotensin II-induced aortic aneurysm and atherosclerosis in apolipoprotein E-deficient mice.* Sci Rep, 2016. **6**: p. 35190.
124. Adada, M., C. Luberto, and D. Canals, *Inhibitors of the sphingomyelin cycle: Sphingomyelin synthases and sphingomyelinases.* Chem Phys Lipids, 2016. **197**: p. 45-59.
125. Kohno, T., et al., *Novel role of copper transport protein antioxidant-1 in neointimal formation after vascular injury.* Arterioscler Thromb Vasc Biol, 2013. **33**(4): p. 805-13.
126. Then, C., et al., *Serum uromodulin and risk for cardiovascular morbidity and mortality in the community-based KORA F4 study.* Atherosclerosis, 2020. **297**: p. 1-7.
127. Zhang, J., et al., *Altered expression of lysosomal hydrolase, acid alpha-glucosidase, gene in coronary artery disease.* Coron Artery Dis, 2016. **27**(2): p. 104-8.
128. Tawa, H., et al., *Role of afadin in vascular endothelial growth factor- and sphingosine 1-phosphate-induced angiogenesis.* Circ Res, 2010. **106**(11): p. 1731-42.
129. Kremen, M., et al., *Plasminogen mediates the atherogenic effects of macrophage-expressed urokinase and accelerates atherosclerosis in apoE-knockout mice.* Proc Natl Acad Sci U S A, 2008. **105**(44): p. 17109-14.
130. Hemdahl, A.L., et al., *Expression of neutrophil gelatinase-associated lipocalin in atherosclerosis and myocardial infarction.* Arterioscler Thromb Vasc Biol, 2006. **26**(1): p. 136-42.
131. Amighi, J., et al., *Beta 2 microglobulin and the risk for cardiovascular events in patients with asymptomatic carotid atherosclerosis.* Stroke, 2011. **42**(7): p. 1826-33.
132. Ragolia, L., et al., *Accelerated glucose intolerance, nephropathy, and atherosclerosis in prostaglandin D2 synthase knock-out mice.* J Biol Chem, 2005. **280**(33): p. 29946-55.

133. Sena, B.F., J.L. Figueiredo, and E. Aikawa, *Cathepsin S As an Inhibitor of Cardiovascular Inflammation and Calcification in Chronic Kidney Disease.* Front Cardiovasc Med, 2017. **4**: p. 88.
134. Baeyens, N., et al., *Redundant control of migration and adhesion by ERM proteins in vascular smooth muscle cells.* Biochem Biophys Res Commun, 2013. **441**(3): p. 579-85.
135. Nahon, J.E., M. Hoekstra, and M. Van Eck, *Total body proteoglycan 4 (Prg4) deficiency increases atherosclerosis susceptibility in apolipoprotein E knockout and low-density lipoprotein receptor knockout mice.* Atherosclerosis, 2018. **278**: p. 315-316.
136. Jaisson, S., C. Pietrement, and P. Gillery, *Carbamylation-derived products: bioactive compounds and potential biomarkers in chronic renal failure and atherosclerosis.* Clin Chem, 2011. **57**(11): p. 1499-505.
137. Wang, Q., et al., *Tryptophan-kynurenine pathway is dysregulated in inflammation, and immune activation.* Front Biosci (Landmark Ed), 2015. **20**: p. 1116-43.
138. Pamplona, R., et al., *Proteins in human brain cortex are modified by oxidation, glycoxidation, and lipoxidation. Effects of Alzheimer disease and identification of lipoxidation targets.* J Biol Chem, 2005. **280**(22): p. 21522-30.
139. Nehler, M.R., L.M. Taylor, Jr., and J.M. Porter, *Homocysteinemia as a risk factor for atherosclerosis: a review.* Cardiovasc Surg, 1997. **5**(6): p. 559-67.
140. Chen, S.S., et al., *Sulfur dioxide acts as a novel endogenous gaseous signaling molecule in the cardiovascular system.* Chin Med J (Engl), 2011. **124**(12): p. 1901-5.
141. Lee, S.E. and Y.S. Park, *Korean Red Ginseng water extract inhibits COX-2 expression by suppressing p38 in acrolein-treated human endothelial cells.* J Ginseng Res, 2014. **38**(1): p. 34-9.
142. McGrath, C.E., et al., *Structure-activity analysis of diffusible lipid electrophiles associated with phospholipid peroxidation: 4-hydroxynonenal and 4-oxononenal analogues.* Chem Res Toxicol, 2011. **24**(3): p. 357-70.
143. Nagai, R., et al., *Peroxynitrite induces formation of N(epsilon)-(carboxymethyl) lysine by the cleavage of Amadori product and generation of glucosone and glyoxal from glucose: novel pathways for protein modification by peroxynitrite.* Diabetes, 2002. **51**(9): p. 2833-9.
144. Chuang, W.T., et al., *Benzyl Isothiocyanate and Phenethyl Isothiocyanate Inhibit Adipogenesis and Hepatosteatosis in Mice with Obesity Induced by a High-Fat Diet.* J Agric Food Chem, 2019. **67**(25): p. 7136-7146.
145. Soares, E.S.A.K., et al., *Effect of new thiazolidine derivatives LPSF/GQ-02 and LPSF/GQ-16 on atherosclerotic lesions in LDL receptor-deficient mice (LDLR(-/-)).* Cardiovasc Pathol, 2013. **22**(1): p. 81-90.
146. Liu, A., et al., *Metformin Delays the Development of Atherosclerosis in Type 1 Diabetes Mellitus via the Methylglyoxal Pathway.* Diabetes Ther, 2020. **11**(3): p. 633-642.
147. Becker, D.J. and J.B. Lowe, *Fucose: biosynthesis and biological function in mammals.* Glycobiology, 2003. **13**(7): p. 41R-53R.
148. Hatch, E., et al., *Differential effects of alcohol and its metabolite acetaldehyde on vascular smooth muscle cell Notch signaling and growth.* Am J Physiol Heart Circ Physiol, 2018. **314**(1): p. H131-H137.
149. Heier, M., et al., *The advanced glycation end product methylglyoxal-derived*

hydroimidazolone-1 and early signs of atherosclerosis in childhood diabetes. Diab Vasc Dis Res, 2015. **12**(2): p. 139-45.

150. Chen, X.F., X. Chen, and X. Tang, *Short-chain fatty acid, acylation and cardiovascular diseases.* Clin Sci (Lond), 2020. **134**(6): p. 657-676.
151. Wang, Z., et al., *Nepsilon-carboxymethyl-lysine-induced PI3K/Akt signaling inhibition promotes foam cell apoptosis and atherosclerosis progression.* Biomed Pharmacother, 2019. **115**: p. 108880.
152. Rodgers, K.J. and R.T. Dean, *Metabolism of protein-bound DOPA in mammals.* Int J Biochem Cell Biol, 2000. **32**(9): p. 945-55.